energies

MDPI

Review

A Review of Proton Exchange Membrane Degradation Pathways, Mechanisms, and Mitigation Strategies in a Fuel Cell

Dharmjeet Madhav [1,*], Junru Wang [1], Rajesh Keloth [2], Jorben Mus [3], Frank Buysschaert [3] and Veerle Vandeginste [1,*]

[1] KU Leuven Bruges, Department of Materials Engineering, Surface and Interface Engineered Materials, 8200 Bruges, Belgium
[2] Department of Chemical and Biomolecular Engineering, University of Nebraska-Lincoln, Lincoln, NE 68588, USA
[3] KU Leuven Bruges, Department of Mechanical Engineering, Applied Mechanics and Energy Conversion, 8200 Bruges, Belgium
* Correspondence: dharmjeet.madhav@kuleuven.be (D.M.); veerle.vandeginste@kuleuven.be (V.V.)

Abstract: Proton exchange membrane fuel cells (PEMFCs) have the potential to tackle major challenges associated with fossil fuel-sourced energy consumption. Nafion, a perfluorosulfonic acid (PFSA) membrane that has high proton conductivity and good chemical stability, is a standard proton exchange membrane (PEM) used in PEMFCs. However, PEM degradation is one of the significant issues in the long-term operation of PEMFCs. Membrane degradation can lead to a decrease in the performance and the lifespan of PEMFCs. The membrane can degrade through chemical, mechanical, and thermal pathways. This paper reviews the different causes of all three routes of PFSA degradation, underlying mechanisms, their effects, and mitigation strategies. A better understanding of different degradation pathways and mechanisms is valuable in producing robust fuel cell membranes. Hence, the progress in membrane fabrication for PEMFC application is also explored and summarized.

Keywords: fuel cells; PEMFC; Nafion; degradation; mitigation strategies

Citation: Madhav, D.; Wang, J.; Keloth, R.; Mus, J.; Buysschaert, F.; Vandeginste, V. A Review of Proton Exchange Membrane Degradation Pathways, Mechanisms, and Mitigation Strategies in a Fuel Cell. *Energies* **2024**, *17*, 998. https://doi.org/10.3390/en17050998

Academic Editors: Lei Xing and Željko Penga

Received: 22 January 2024
Revised: 10 February 2024
Accepted: 17 February 2024
Published: 20 February 2024

1. Introduction

Rapid population growth and industrialization requiring enormous amounts of fossil fuels-based energy have led to excessive emissions of greenhouse gases, mainly CO_2, causing severe environmental issues. Recent environmental awareness and stringent governmental policies have forced the world to transition from quickly depleting and pollution-causing fossil fuel-based energy to green and alternative renewable sources of energy. Hence, researchers are exploring greener alternative sources of energy [1,2] and, at the same time, possible ways to utilize the CO_2 emission streams [3–5]. There are several sources of energy, such as wind, solar, geothermal, and hydropower, that are greener and renewable. Nevertheless, the intermittent nature and unpredictability of these sources present significant challenges to ensuring their stable operation as reliable energy sources for end users. Fuel cells, which are electrochemical devices that can convert the chemical energy stored in a fuel into electrical energy without actual fuel combustion, could be a potential solution. Depending on the nature of the electrolyte used, fuel cells can be categorized as polymer electrolyte (proton exchange) membrane fuel cells (PEMFCs), phosphoric acid fuel cells (PAFCs), molten carbonate fuel cells (MCFCs), direct methanol fuel cells (DMFCs), alkaline fuel cells (AFCs), and solid oxide fuel cells (SOFCs) [6,7]. Proton exchange membrane fuel cells (PEMFCs), which convert the chemical energy of hydrogen that can be produced using renewable energy sources such as solar, wind, etc., into electrical energy, have the potential to tackle the issues originating from the intermittent and unpredictable nature of renewable sources [8]. Features such as high compactness,

high power density, noiseless operation, and efficient energy production without releasing pollutants or CO_2 make PEMFCs a promising cleaner energy source [9].

PEMFCs mainly consist of membrane–electrode assembly (MEA), bipolar plates, and sealing gaskets in a sandwich structure (Figure 1a). A fuel cell stack is formed by several MEAs, and each MEA is sandwiched between two bipolar plates, providing a foundation and mechanical support by acting as a shield to the fuel cell. Gaskets are added around the edges of the MEA to prevent any gas leaks. The electrochemical reaction takes place at the MEA, which is composed of an anode and a cathode, each containing a gas diffusion layer and an active catalyst layer separated by a proton exchange membrane (PEM). Hydrogen is injected as fuel on the anode side and diffuses through the gas diffusion layer to reach the anode catalyst layer. The catalyst facilitates hydrogen oxidization to produce protons (H^+) and electrons (e^-) (1). The proton exchange membrane allows protons to pass through to reach the cathode catalyst layer while electrons are transferred to the cathode via an external circuit. Air is injected on the cathode side and reaches the cathode catalyst layer, flowing through the gas diffusion layer. The cathodic catalyst enables oxygen reduction by reacting with the protons that have crossed the membrane and electrons available from the external circuit (2), producing water and heat using H_2 and O_2 in the overall process (3) (Figure 1b).

$$\text{Anode reaction}: \ H_2 \rightarrow 2H^+ + 2e^- \quad (1)$$

$$\text{Cathode reaction}: \ O_2 + 4H^+ + 4e^+ \rightarrow 2H_2O \quad (2)$$

$$\text{Overall reaction}: \ 2H_2 + O_2 \rightarrow 2H_2O \quad (3)$$

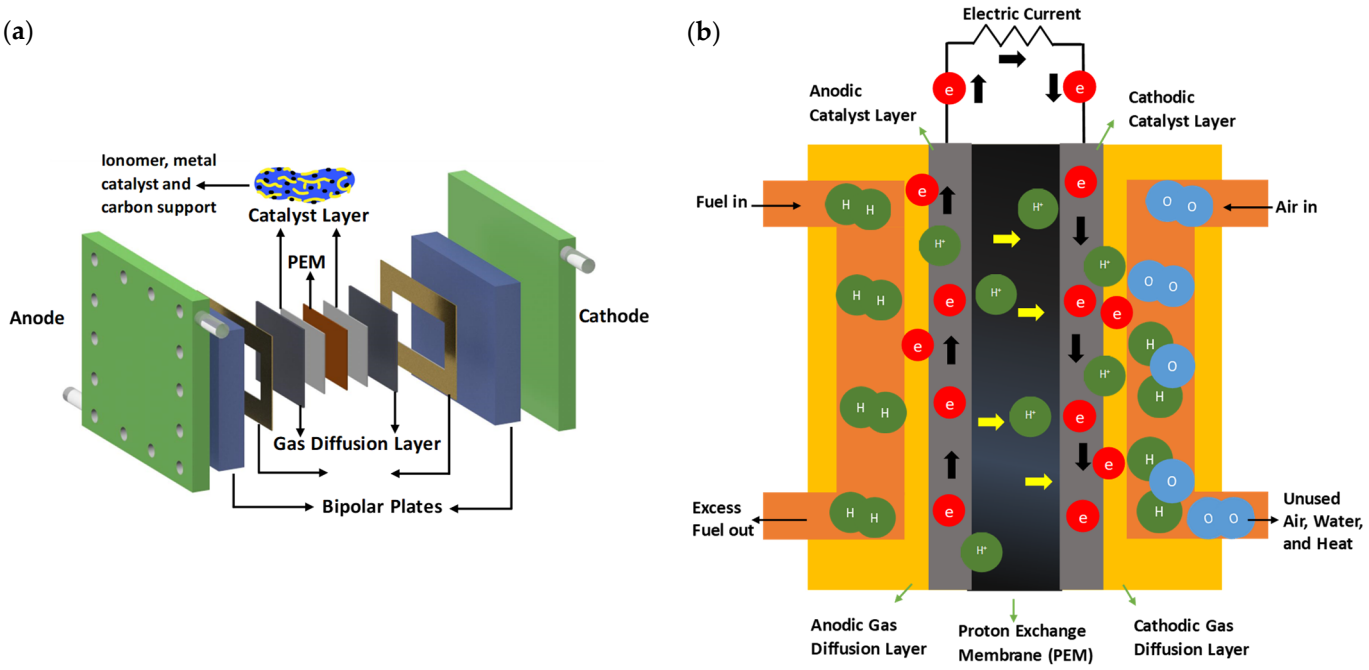

Figure 1. (**a**) Schematic showing the components of a PEMFC: bipolar plates, sealing gaskets, gas diffusion layers, catalyst layers, and the proton exchange membrane; this arrangement is repeated in a fuel cell stack. (**b**) Description of the operation of a PEMFC.

The proton exchange membrane is the key element of the PEMFC, as it must permit only the protons to pass while preventing direct electron conduction and gas permeation between the anode and cathode. Such a requirement makes it essential for PEM to have excellent proton conductivity and extremely low gas and electron permeability. Furthermore, PEMFCs are operated in harsh working conditions integrating water, air, hydrogen, and heat, necessitating the PEM to have sufficient chemical, mechanical, thermal, and dimensional stability [10]. Several polymers have been considered as PEMs for their application

in PEMFCs under diverse operating conditions [11–14]. They can be mainly categorized as non-fluorinated and fluorinated polymeric membranes. The latter has been preferred because most non-fluorinated membranes, although having attractive prices, have poor resistance to oxidation and undergo thermal degradation. Fluorinated proton exchange membranes, especially fully fluorinated (perfluorinated) ones, have the advantageous combination of chemical, thermal, mechanical, and dimensional stability.

Nafion, a perfluorosulfonic acid membrane, was developed in the mid-1960s by DuPont and is the most used PEM in PEMFCs. It consists of an aliphatic perfluorocarbon hydrophobic chain and hydrophilic sulfonic acid terminated perfluoro vinyl ether side groups that exhibit excellent proton conductivity and good chemical, oxidative, and dimensional stability [15]. However, it has been found that PEM degradation is one of the significant issues in the long-term operation of PEMFCs. The membrane degradation can lead to a decrease in fuel cell performance and a shorter lifespan. While Nafion has been a dominant proton exchange membrane, several polymers with similar core structures, such as Aquivion® and Hyflon® (earlier DOW) by Solvay (Brussels, Belgium), Flemion® by Asahi Glass, (Chiyoda City, Tokyo, Japan) and Dyneon™ by 3M (Saint Paul, MN, USA), etc. (Figure 2), have been studied as PEMs in fuel cells [16,17]. Given their similar core structures, the degradation issue is analogous to that of Nafion; therefore, the discussions in this review could be applied to all similar polymers.

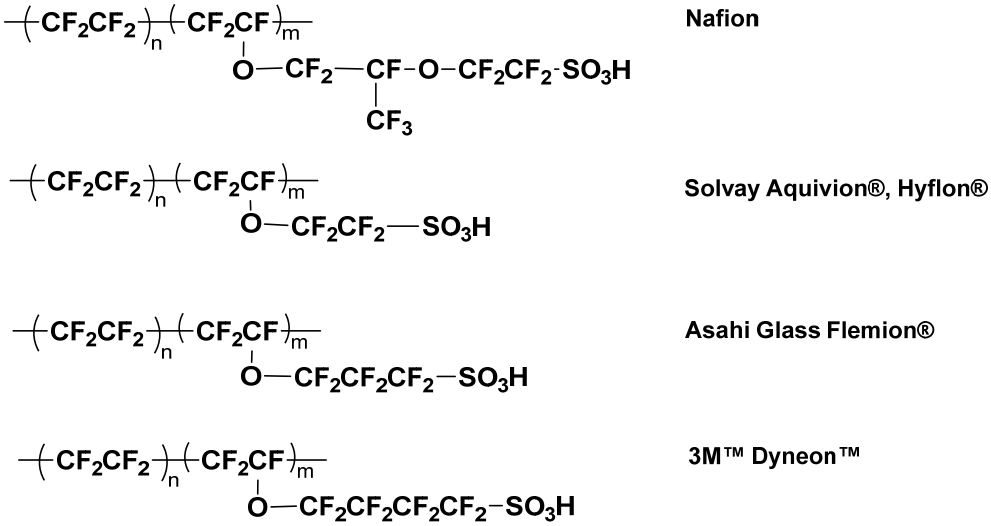

Figure 2. Chemical structures of some commercial perfluorosulfonic acid-based proton exchange membranes.

The different pathways for PFSA membrane degradation in PEMFCs can be classified into chemical, thermal, and mechanical degradation. We review various causes leading to each route of degradation, the underlying mechanisms, and mitigation strategies. Furthermore, we analyze the progress in membrane fabrication processes for PEMFC applications.

2. Chemical Degradation

The chemical degradation of a proton exchange membrane can be triggered by metal poisoning, impurities in the fuel and the air streams, and radical attack on the polymer structure. Each of these causes, along with the degradation mechanisms, are discussed next. Finally, at the end of the section, overall mitigation strategies for chemical degradation are explored.

2.1. Metal Poisoning

There are two main sources of undesired metal contaminants in the fuel cell system: (i) impurities in fuel streams or humidifier sources and (ii) corrosion of the metal bipolar plates [18,19]. Metal ions can affect the performance of membranes in two ways. First,

several metal cations have a stronger affinity to the sulfonic acid groups of membranes than H^+. Consequently, a significant number of active sites are occupied by undesired cations during fuel cell operation, negatively affecting the membrane ionic conductivity, hydration, and H^+ transfer rate [20,21]. When hydrogen is produced from water, it may contain cations such as Ca^{2+} and Na^+ in the fuel stream [22,23]. The same applies to the air stream; it may contain several impurities depending on the site of operation. For example, the air in a sea region or industrial area may contain extremely high concentrations of Na^+ or airborne particulate matter, respectively [24,25]. The second effect of metal ion contaminants is the catalysis of the radical formation reaction, discussed in Section 2.3.

Some common metal ion impurities that can originate from water in the humidifier, fuel streams, metal alloy components, or alloy catalysts of the fuel cell system include Fe^{3+}, Fe^{2+}, Ca^{2+}, Cu^{2+}, Na^+, Li^+, K^+, Mg^{2+}, Ni^{2+}, Co^{2+}, Cr^{3+}, and Al^{3+} (Table 1) [26,27].

Table 1. Metal ion contaminant sources.

Typical Pollutant	Sources
Ions of Fe, Cr, Ni, Mo, Mn, Cu	Metal bipolar plates
Ions of Ca, Na	Membrane, gaskets, fuel
Ions of Si, Ca, Mg, K	Gaskets
Ions of Si, Na, Ca, Mg, Al, S, K, Fe, Cu, V, Cr	Coolants, DI water

Each metal ion affects the fuel cell performance and membrane degradation differently. The presence of 5 ppm Fe^{3+} in the air stream resulted in the fuel cell performance decline of 174 mV within 191 h, whereas the presence of 5 ppm Al^{3+} led to a degradation of only 65 mV over a span of 282 h. The stronger effect of Fe^{3+} was attributed to its catalytic effect in the production of radicals, causing the formation of pinholes in the membrane, evidenced by the sudden death of the fuel cell during tests and based on scanning electron microscopy (SEM) analysis [28]. However, another study reported the ranking of four metal cations in terms of the greatest reduction in fuel cell performance as $Al^{3+} \gg Fe^{2+} > Ni^{2+}$, Cr^{3+} when membranes were contaminated by immersion in metal sulfide solutions before use in the fuel cells [29]. This suggests that the procedure of contamination introduction in the fuel cell itself has a significant impact. Ca^{2+} is present in water in considerably high concentrations, making it an inevitable impurity in air humidifier streams. The injection of 5 ppm and higher Ca^{2+} in the air stream led to large cell performance degradation at 1 A cm^{-2} with severe membrane degradation, whereas at 0.6 A cm^{-2}, only a slight performance loss was observed with the same level of impurity. Furthermore, precipitation of $CaSO_4$ significant enough to induce mass transport resistance was observed between the gas diffusion layers and bipolar plates of the cathode at all test conditions, even at lower Ca^{2+} concentrations of 2 ppm [30,31]. Moreover, Ca^{2+} causes a reduction in the O_2 permeability by being absorbed in the perfluorinated ionomer in the gas diffusion layer [32]. Mg^{2+}, which is also a common metal cation found in water streams and could leach from bipolar plates and elastomeric gaskets degradation, decreases the voltage and maximum power density of the fuel cell with an increase in Mg^{2+} concentration and contamination time [33,34]. Qi et al. investigated the effects of K^+, Ba^{2+}, Ca^{2+}, and Al^{3+} by in situ injection of cationic salt solutions with ClO_4^- anions in the air stream [35]. The degradation in cell performance in the presence of metal ion contaminants was attributed to the increase in mass transport resistance and the decrease in the electrochemical surface area caused by the replacement of protons on the sulfonate groups. Another study revealed that higher valence cations exhibit stronger interactions and a higher affinity for sulfonic sites compared to lower valence cations [36]. The replacement of H^+ with metal cations causes physical deterioration of the membrane, such as shrinkage and density increment [37]. Furthermore, the presence of cations decreases the water content, ionic conductivity, H^+ transference, and water permeability proportionally to the number of cations. Metal cations affect not only the membrane but also the catalyst/support and ionomer. Lee et al. [38] found that Co^{2+} contamination has a negative impact on ionomer conductivity and oxygen

transport through the catalyst layer. They discovered that when the membrane area is large compared to the active area being used in MEA, Co^{2+} migrates to the inactive membrane area, acting as a Co^{2+} sink and resulting in a negligible effect of Co^{2+} on performance. However, when the inactive area was decreased to the proximity of the active area, the performance remained unaffected only up to ~44% of Co^{2+} exchange for a 25 µm thick membrane with an active area of 5 cm^2 in the total membrane area of 8.6 cm^2 [38]. The performance reduction was attributed to increased O_2 and proton transport resistance due to reduced water uptake and availability of sulfonic acid groups (Figure 3).

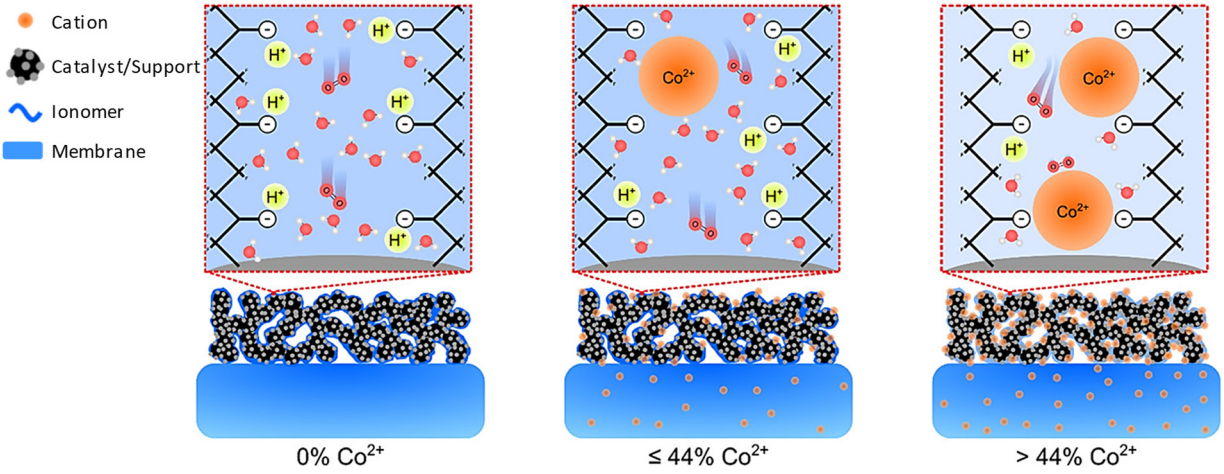

Figure 3. Cation contamination above critical Co^{2+} exchange reduces the water uptake and availability of sulfonic acid groups, negatively influencing the O_2 and H^+ transport. Adapted from [38].

Molecular dynamics (MD) simulations have provided new insights into the mechanisms of metal cation-induced membrane or fuel cell performance degradation. MD simulations have confirmed that Co^{2+} contamination reduces water content and increases the modulus of the ionomer film covering the catalyst surface while reducing the distance between the sulfonic acid groups and increasing the aggregation size of the ionomer [39]. In addition to the effect on membranes, studies suggest that some cationic contaminants prefer to be more concentrated on the cathode side of the PEM when current is drawn through the PEM. Kienitz et al. [40] modeled the effect of Na^+ and Ca^{2+} by solving the Nernst–Planck equation and found them to be more concentrated on the cathode side due to the tradeoff between diffusion and migration of contaminants in the membrane. By contrast, Zhu et al. [41] found Cu^{2+} to be accumulated at the cathode due to the electric field through the thickness direction of the MEA. As indicated in several experimental studies, MD simulations revealed that the diffusion coefficients of H_3O^+ and H_2O are significantly reduced by the presence of Na^+ and Ca^{2+}, with Ca^{2+} having more adverse effects. Moreover, cations affected intramembrane transport properties by occupying sulfonic groups and disrupting the connectivity of water clusters [42]. Conforming observations were made in our previous work where sodium ions replaced hydrogen ions in degraded Nafion fragments, and the rate of substitution increased with increasing temperature [24]. The synergetic effect of metal ions and air pollutants is even more devastating, as it was found to accelerate the degradation of stack performance [43].

2.2. Impurities in the Fuel and Air Streams

The air stream and hydrogen fuel stream expose the fuel cell components to several pollutants that can vary greatly in concentration depending on the sources and location of operation. The primary method for hydrogen production involves reforming hydrocarbons or oxygenated hydrocarbons, such as methane from natural gases and methanol from biomass. The reforming process, which includes steam reforming, autothermal reforming, and partial oxidation, dominates over alternative methods, like fermentation or partial

oxidation of biomass and water electrolysis [22]. However, the reformation of hydrogen from hydrocarbon fuels introduces inevitable impurities such as carbon oxides (CO_2 and CO) and sulfur compounds (H_2S and sulfur organics). Typically, the reforming process generates a hydrogen-rich gas known as "reformate", containing approximately 40 to 70% H_2, 15 to 25% CO_2, 1 to 2% CO, along with small amounts of inert gases (nitrogen and water vapor) and sulfur impurities [26]. Additionally, using ammonia as a tracer gas in natural gas distribution systems can result in the presence of NH_3 and HCN in the reformate. Furthermore, hydrogen production from different fuels leads to the presence of several hydrocarbons, oxygenated hydrocarbons, and odorants. In alternative hydrogen productions, the biomass-based process involves gasification, pyrolysis, conversion to liquid fuels by supercritical extraction, liquefaction, and hydrolysis of biomass, followed in some cases by reformation and biological hydrogen production. The main impurities in biomass-sourced hydrogen are aldehydes, alcohols, acetic acid, formic acid, NH_3, H_2S, and HCN. Hydrogen production from water is a mature and traditional hydrogen production method with commercial uses dating back to the 1890s [22]. There are three main ways to generate hydrogen from water: electrolysis, thermolysis, and photoelectrolysis, and the impurities are the ions from water, such as Ca^{2+}, Na^+, and Cl^-. Table 2 summarizes the different contaminants and their sources in the hydrogen stream. For optimal fuel cell performance and longevity, a purer form of hydrogen is required as the fuel feed. To achieve the necessary purity levels, separation processes are essential for removing undesired impurities from the reformate gas. Despite their effectiveness, these processes are associated with high costs. Filtration, especially for trace amounts of CO and sulfur compounds, poses an even greater challenge and comes with a higher price tag.

Table 2. Sources of different contaminants in the fuel stream.

Typical Pollutants in Hydrogen	Hydrogen Sources
CO, NH_3, H_2S, HCN	Crude oil, natural gas
Hydrocarbons, aldehydes	Gasolines
Mercaptans	Diesels
CO, odorants, alcohols	Methanol/dimethyl ether
Cations, aldehydes, alcohols, formic acid, NH_3, H_2S, HCN	Biomass
CO, CO_2, SO_2, NH_3, H_2S, benzene	Industrial by-products
Ions of Ca, Na, Cl	Water

CO, H_2S, NH_3, and hydrocarbons are considered the main impurities entering the fuel cell system through the hydrogen stream. These contaminants can enter the MEA structure, poisoning the catalyst sites and altering membrane properties, such as hydrophobicity and hydrophilicity and proton transportation routes, and disturbing water management, thus causing performance decay [26]. Although these contaminants mostly cause catalyst poisoning, we discuss the associated effect on the membrane. For example, CO and H_2S interact strongly and are adsorbed on the metal anode catalyst surface, drastically reducing the available active catalyst sites for H_2 electro-oxidation, an essential step for fuel cell operation [44–46]. Increasing the operating temperature is one of several catalyst poisoning mitigation strategies [45]. However, Nafion and similar membranes need to be hydrated for proton transport, limiting the operating temperature to below 90 °C. Increasing operating temperatures to tackle the catalyst poisoning may lead to dehydrated and mechanically damaged membranes, causing performance loss. NH_3, as a fuel contaminant, has a more prominent and direct effect on the membrane. Gomez et al. [47] studied the effect of NH_3 on each fuel cell components and overall performance. They found that NH_3 severely degrades the overall fuel cell performance by affecting the membrane conductivity, catalyst ionomer of both electrodes, the hydrogen oxidation reaction, and the oxygen reduction reaction. Zhang et al. [48] found that the effect of NH_3 on the membrane is more intense than that on the electrodes. The electrochemical impedance spectroscopy (EIS) results at a relative humidity (RH) of 49% for both the anode gas and the cathode gas streams

revealed that the high-frequency response increases gradually, indicating an increase in membrane resistance due to contamination (Figure 4a). The recovery test indicated that membrane resistance can only recover about 60% (Figure 4b), which appears to be more permanent damage compared to electrodes. It has been speculated by several researchers that the membrane and ionomer conductivity reduction could be due to NH_4^+ formation ($NH_3 + H^+ \rightarrow NH_4^+$), which can occupy the charged sites of the PEM [47–49]. Furthermore, like CO and H_2S, NH_3 adsorption onto metal catalysts (mostly Pt) may block H_2 oxidation at the anode and, similarly, the oxygen reduction reaction at the cathode catalyst by crossing over to the cathode side [23].

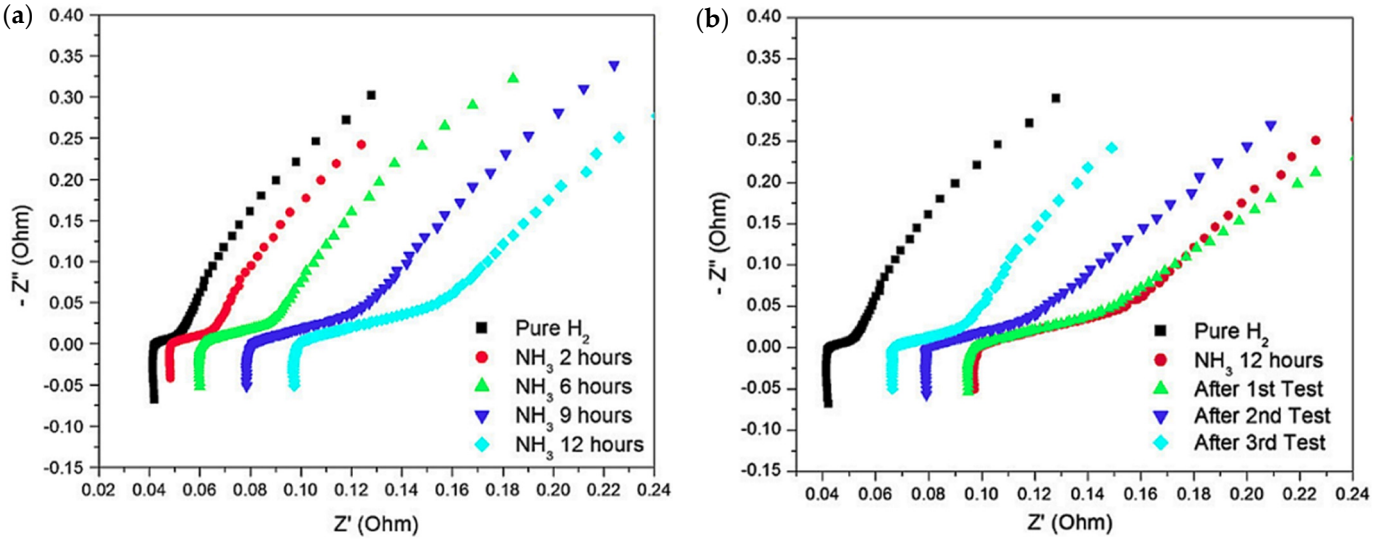

Figure 4. Electrochemical impedance spectroscopy measurement at RH 49%, sweep frequency 10000—0.1 Hz, amplitude 10 mV (**a**) during the contamination processes; (**b**) during the recovery test. Adapted with permission from [48].

Hydrocarbon impurities in the fuel stream do not generally have a drastic effect on fuel cell performance or membrane stability. Therefore, the studies have also been limited. Common hydrocarbon methane is believed to have no poisoning effect, while formaldehyde (HCHO) and formic acid (HCOOH) show a very small and reversible catalyst poisoning effect [50]. Methanol in the hydrogen stream, depending on its concentration and exposure time, results in reversible degradation in the performance of the PEMFC [51]. The poisoning effect of methanol at low concentrations, up to 200 ppm, is reversible, and beyond that, it takes a very long time to recover. Another study determined that 5 ppm HCHO, 2 ppm HCOOH, 19 ppm chloromethane, 30 ppm acetaldehyde, 5% ethylene, 20 ppm toluene, and 10 ppm benzene do not lead to significant degradation of the fuel cell when present individually in the fuel stream [52]. Furthermore, up to a certain concentration, a mixture of CO, H_2S, HCOOH, benzene, and ammonia does not significantly affect fuel cell performance. Overall, hydrocarbon impurities, in some cases, affect the fuel cell performance; however, the effect on membrane stability is not clear yet. The effects of cations are analogous to what has been discussed in Section 2.1.

The air stream is the most convenient way to feed oxygen to fuel cells. However, ambient air, depending on the location, contains several impurities that are detrimental to the fuel cell membrane electrode assembly and overall performance [53]. Nitrogen oxides (NO and NO_2), carbon oxides (CO and CO_2), sulfur oxides (SO_2 and SO_3), O_3, hydrocarbons, soot, and particulates are common pollutants originating from fossil fuel combustion. Considerable amounts of NH_3, ions of salts, and dust are present in ambient air in farming areas, seaside, and industrial zones, respectively. De-icers and humidifiers introduce several metal cations into the fuel cell system. Other air impurities that can be

encountered are chemical warfare agents, including SO_2, NO_2, CO, propane, and benzene present on a battlefield. Table 3 lists the different air contaminants and their sources.

Table 3. Sources of different contaminants in air stream.

Typical Pollutants in Air	Sources
SO_x, NO_x, CO_x, O_3, hydrocarbons, soot, particulates	Fuel combustion, pollution
NH_3	Ambient air, farming
Cations and anions from ocean salts, dust	Natural sources
Ions of Na, Ca, Mg, Al, K, Fe, Cu, V, Cr, Cl	De-icers, humidifiers
SO_2, NO_2, CO, propane, benzene	Battlefield pollutants

The contaminants in the air stream that are similar in nature to those in the fuel stream have similar effects, i.e., the poisoning of the catalyst on the cathode side and influencing the oxygen reduction reaction, and if they cross the membrane, they affect H_2 oxidation on the anode side. Other contaminants that are not present in the fuel stream also have an analogous effect. For instance, exposure to NO and NO_2 leads to a current drop even at concentrations of 1 ppm [54]. However, the effects are reversible and even faster at elevated temperatures. Another study reported the reversibility of the NO_2 impact until at least 4 ppm, which is much higher than the NO_2 concentration that can be encountered in real PEMFC operations [55]. Misz et al. [56] conducted a systemic review of the effect of different air contaminants on fuel cells and experimentally investigated the effects of NO, NO_2, SO_2, NH_3, toluene, and ethane. Contamination caused a significant degradation in performance, mostly due to the effect on the cathode with the possibility of regeneration. PEM is mainly affected by two types of species that can originate from air impurities, namely NH_4^+ and metal cations [43,57]. The effect of metal cations on membranes has been discussed in Section 2.1. NH_4^+ can originate in fuel cell systems through different paths. One route has been discussed above, where NH_3 enters the anode side as a fuel impurity and can react with H^+ to form NH_4^+, occupying the charged sites. A similar reaction can occur when NH_3 enters the fuel cell as an air impurity, causing the same issue of reduced membrane conductivity. The other route of NH_4^+ formation is through the reduction of NO_x impurities according to Reactions (4) and (5).

$$NO_2 + 8H^+ + 7e^- \rightarrow NH_4^+ + 2H_2O \quad (4)$$

$$NO + 6H^+ + 5e^- \rightarrow NH_4^+ + 2H_2O \quad (5)$$

NH_4^+ has several detrimental effects on the membrane. Hongsirikarn et al. [58] compared the conductivities of Nafion membranes with different NH_4^+ concentrations in deionized water at room temperature and in a gas phase at 80 °C at various relative humidities. The conductivity in the water phase decreased linearly with an increase in the NH_4^+ concentration in the membrane, with a 75% decrease in conductivity for the fully exchanged NH_4^+ form compared to the membrane, with SO_3^- groups fully occupied by H^+. By contrast, depending on humidity, the gas phase conductivity of the NH_4^+ form exhibited a reduction ranging from 66% to 98% compared to the H^+ form. The conductivity of a cation generally decreases with an increase in its radius [59]. The Pauling cation radius of NH_4^+ (~1.52 Å) is approximately four times larger than that of H^+ (~0.4 Å), which explains the drastic decrease in membrane conductivity once H^+ is exchanged with NH_4^+. Furthermore, membrane thinning due to NH_4^+ uptake was observed, which is possibly caused by the formation of hydrogen bonds by a lone pair of electrons of nitrogen and of hydrogen in the N–H bond with adjacent water molecules (H–N···H–O–H, N–H···H–O–H) and thus a tighter, more compact structure formation [58]. Furthermore, SO_2 and NO_2 in the air stream are dissolved into water and generate H_+, SO_4^{2-}, and NO_3^-, reducing the pH of the water on the surface of the alloy bipolar plates [43]. Reduced pH leads to accelerated corrosion of the air outlet at the end plate, which may result in metal ion contaminants known to accelerate membrane degradation. Recently, there has been tremendous interest in using

fuel cells for military applications, which raises concerns due to battlefield pollutants [60]. Moore et al. [61] investigated the impact of chemical warfare agents, sarin, sulfur mustard, cyanogen chloride, and hydrogen cyanide on PEMFC performance. All chemical warfare agents tested seriously compromised the performance of the fuel cells irreversibly.

2.3. Radical Attack

The degradation of PEM due to radical attack is the most disastrous for fuel performance and longevity, as it dismantles the fluorocarbon backbone in membranes, affecting the proton conductivity and mechanical strength [24,62]. Radical attack on the membrane is considered the most prominent reason for membrane chemical degradation. Oxygen molecules from the air stream permeate the membrane from the cathode side and are reduced at the anode metal catalyst to form hydrogen peroxide via reactions (6)–(8).

$$H_2 + Pt \rightarrow Pt\text{-}H \text{ (at anode)} \quad (6)$$

$$Pt\text{-}H + O_2 \text{ (permeated through PEM)} \rightarrow \bullet OOH \quad (7)$$

$$\bullet OOH + Pt\text{-}H \rightarrow H_2O_2 \quad (8)$$

H_2O_2 is a very reactive species; however, H_2O_2 itself is not a capable oxidant to substantially damage the polymer structure [63]. In fact, perfluorosulfonic acid membranes are stable against 30% H_2O_2 up to 80 °C in the absence of metal ions or other sources generating radicals, such as UV light [64]. Contamination by trace metal ions, mainly Fe^{2+}, Cu^{2+}, and other multivalent cations like Cr^{2+} or Ti^{3+} originating from different sources (Table 1), catalyze the decomposition of H_2O_2 to produce hydroxyl (•OH) (9) and hydroperoxyl (•OOH) (10) radicals. •OH can further react with H_2 to generate •H (11) [65].

$$H_2O_2 + M^{x+} \rightarrow M^{(x+1)+} + \bullet OH + OH^- \quad (9)$$

$$\bullet OH + H_2O_2 \rightarrow H_2O + \bullet OOH \quad (10)$$

$$\bullet OH + H_2 \rightarrow H_2O + \bullet H \quad (11)$$

The produced radicals attack and degrade the membrane in several ways. In situ membrane degradation is tested by open circuit voltage hold testing [66], while the Fenton reagent, consisting of hydrogen peroxide and ferrous ions, is employed to study the membrane degradation ex situ [24]. The ex situ investigations give better insight into the degradation behavior of PEM under different conditions that can be mimicked precisely. There are four vulnerable sites in perfluorosulfonic acid membranes where these radicals can attack [67]. The first is the carboxylic acid end groups, which are inevitably generated during the polymer manufacturing process or through the transformation of other non-perfluorinated end groups via radical attack [68]. The highly unstable radicals formed through the reactions described above (9) and (10) attack the carboxylic groups to produce CO_2, HF, and a perfluorocarbon radical (12) (Figure 5) [69]. The produced perfluorocarbon radical reacts with another •OH to form an acid fluoride and HF (13) and (14). Finally, the acid fluoride undergoes hydrolysis to generate carboxylic acid end groups in the polymer chain with one carbon removed (15). The carboxylic acid end group generation makes this mode of degradation continuous, with each cycle removing one carbon from the chain, resembling the unzipping process. When all carbons before the side chain (m) become unzipped through this process, the degradation product CO_2H–$CF(CF_3)$–O–CF_2–CF_2–SO_3H is produced, which may further decompose to HO–CF_2–CF_2–SO_3H and trifluoroacetic acid due to •OH attack on the ether bond [70]. Furthermore, the degradation product itself can undergo a further unzipping process starting from the carboxylic acid group and produce HOOC–CF_2–SO_3H and trifluoroacetic acid [71]. A recent study has

found evidence of chemical degradation via the unzipping process due to radical attack, observing weight loss, fluoride, and CO_2H–$CF(CF_3)$–O–CF_2–CF_2–SO_3H emissions [72].

$$R\text{-}(CF_2)_mCOOH + \bullet OH \rightarrow R-CF_2\bullet + CO_2 + H_2O \quad (12)$$

$$R-(CF_2)_{m-1}CF_2\bullet + \bullet OH \rightarrow R-(CF_2)_{m-1}CF_2OH \quad (13)$$

$$R-(CF_2)_{m-1}CF_2OH \rightarrow R-(CF_2)_{m-1}COF + HF \quad (14)$$

$$R-(CF_2)_{m-1}COF + H_2O \rightarrow R-(CF_2)_{m-1}COOH + HF \quad (15)$$

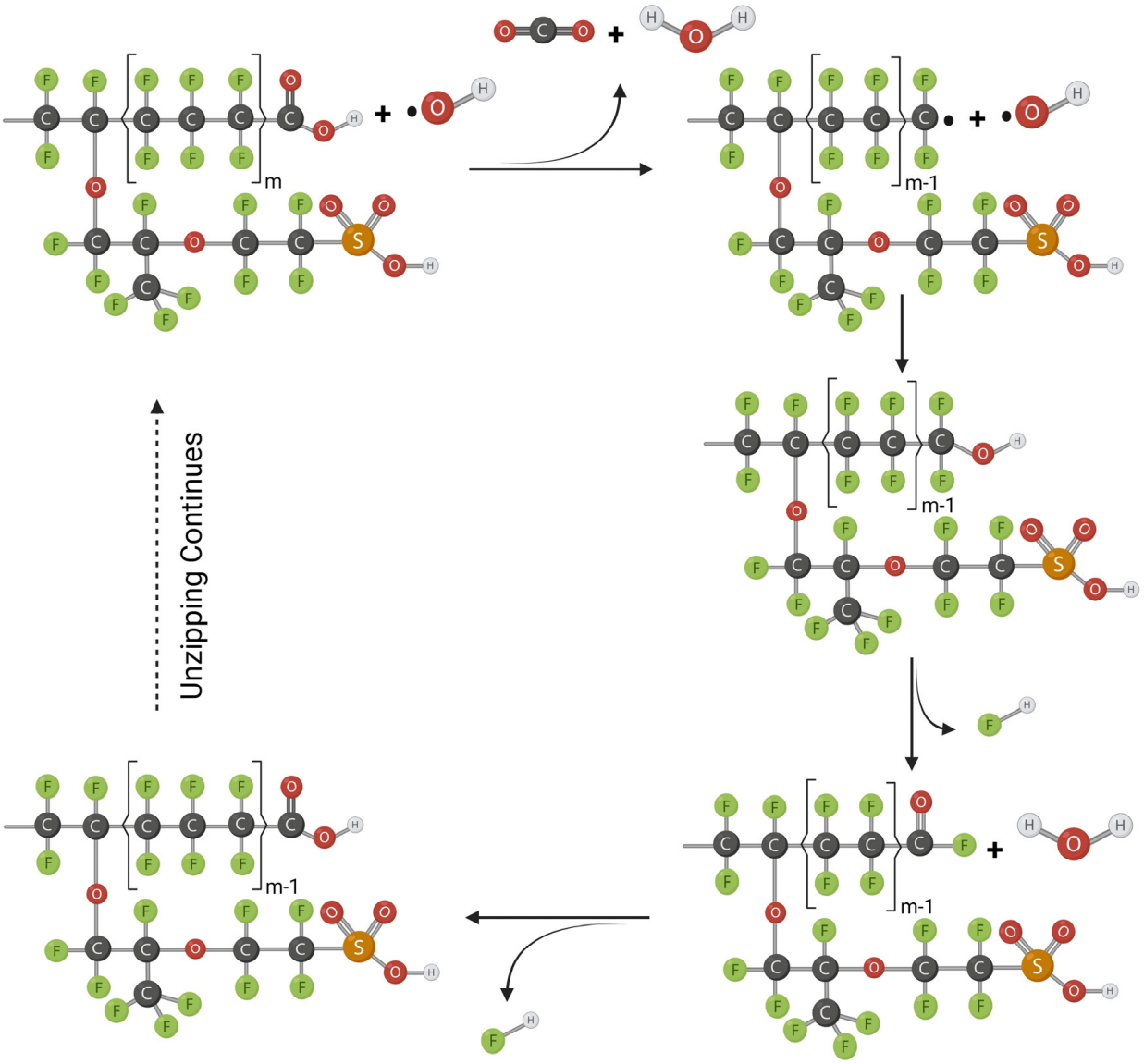

Figure 5. Main chain unzipping mechanism: radical attack on carboxylic acid groups.

Mittal et al. [73] found that the presence of sulfonic acid groups occupied by H^+ in the polymer side chain significantly affects the fluoride emission rate and hence membrane degradation. If the sulfonic acid group is occupied by metal cations instead of H^+, the fluoride emission rate decreases by two orders of magnitude, suggesting the significant role of sulfonic acid groups in membrane degradation. Consequently, the second vulnerable site in the polymer chain is the C–S bond at the end of the side chain. The •OH radical attacks the C–S bond of the side chain, which is also the weakest bond within this segment [74].

In the first step, SO_3, H_2O, and perfluorocarbon radicals are produced (16), and from there, polymer degradation proceeds similarly to the unzipping mechanism (17)–(19), progressively shortening the side chain with HF and CO_2 formation (Figure 6). The detection of $–O–CF_2–CF_2•$ radicals after a UV-induced Fenton test of Nafion and Dow perfluorinated membranes aligns with this degradation mechanism [75].

$$R\text{-}O\text{-}CF_2\text{-}CF_2\text{-}SO_3H + •OH \rightarrow R\text{-}O\text{-}CF_2\text{-}CF_2• + SO_3 + H_2O \quad (16)$$

$$R\text{-}O\text{-}CF_2\text{-}CF_2• + •OH \rightarrow R\text{-}O\text{-}CF_2\text{-}CF_2OH \quad (17)$$

$$R\text{-}O\text{-}CF_2\text{-}CF_2OH \rightarrow R\text{-}O\text{-}CF_2\text{-}COF + HF \quad (18)$$

$$R\text{-}O\text{-}CF_2\text{-}COF + H_2O \rightarrow R\text{-}O\text{-}CF_2\text{-}COOH + HF \quad (19)$$

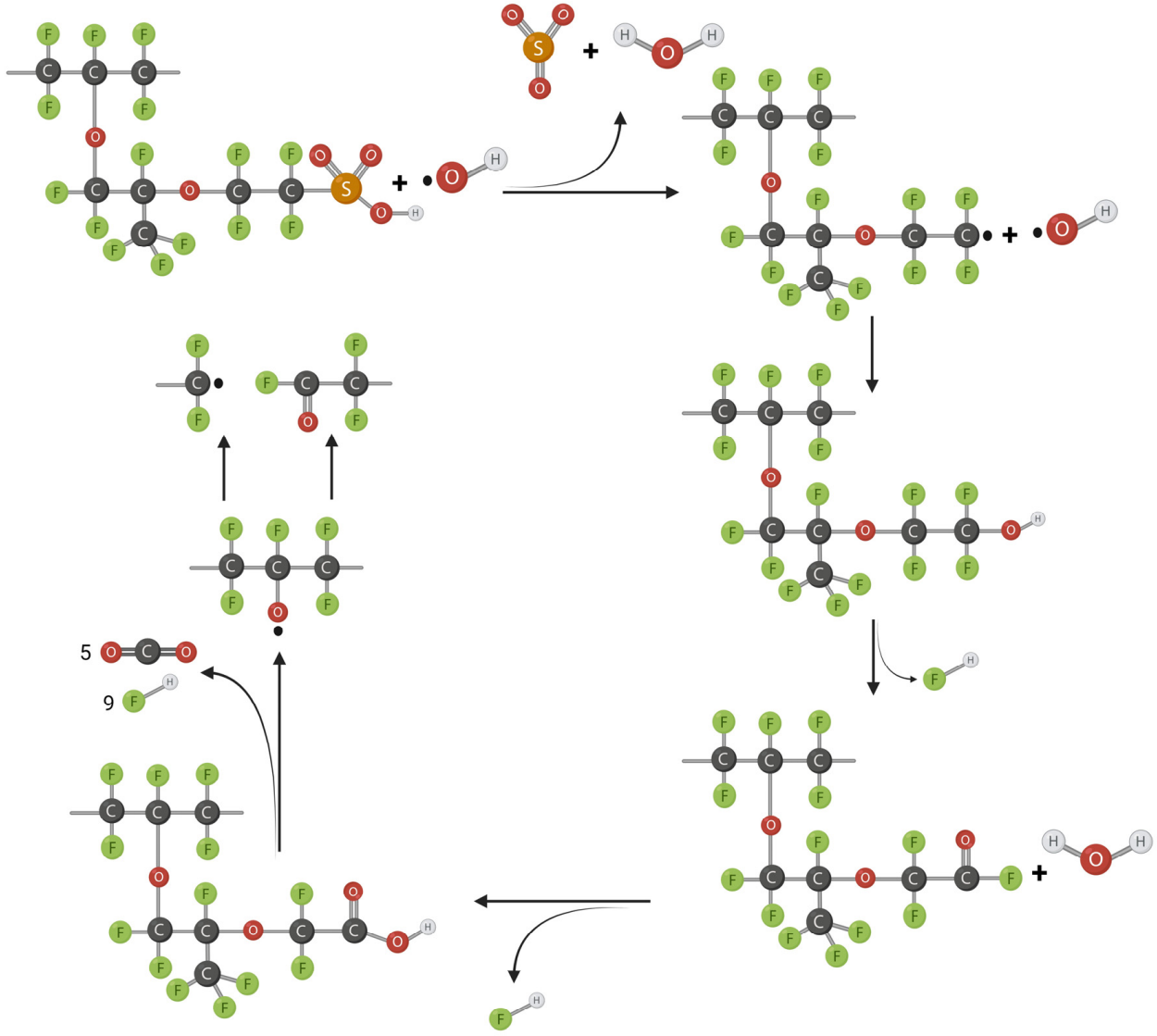

Figure 6. Side chain unzipping mechanism: radical attack on C–S bond.

Tertiary C-F bonds are the most susceptible to radical attack among the fluorocarbons because they have the lowest bond strength [76]. The side chain degradation or main chain scission may also start at the tertiary carbon in the main chain or the tertiary carbon between two ether groups within the side chain. These reactions can lead to complete or partial unzipping of the side chains, releasing HF [74]. The •H removes the fluoride

from the tertiary carbon to produce HF and tertiary carbon radical (Figure 7) [76]. The tertiary carbon radical reacts with 2 •OH to release H_2O and a fragment of the main chain while producing a carbonyl at the tertiary carbon. Carbonyl at the tertiary carbon converts the ether linkage between the main and side chain to the ester group, which undergoes hydrolysis to produce two fragments, the main chain with a carboxylic acid end group and the side chain with an alcohol group. The side chain fragment further reacts with water to release 2 HF while generating the carboxylic acid end group on the side chain as well. The degradation through this mechanism releases a relatively low amount of fluoride; nevertheless, an increase in COOH groups is observed, which can lead to degradation by unzipping.

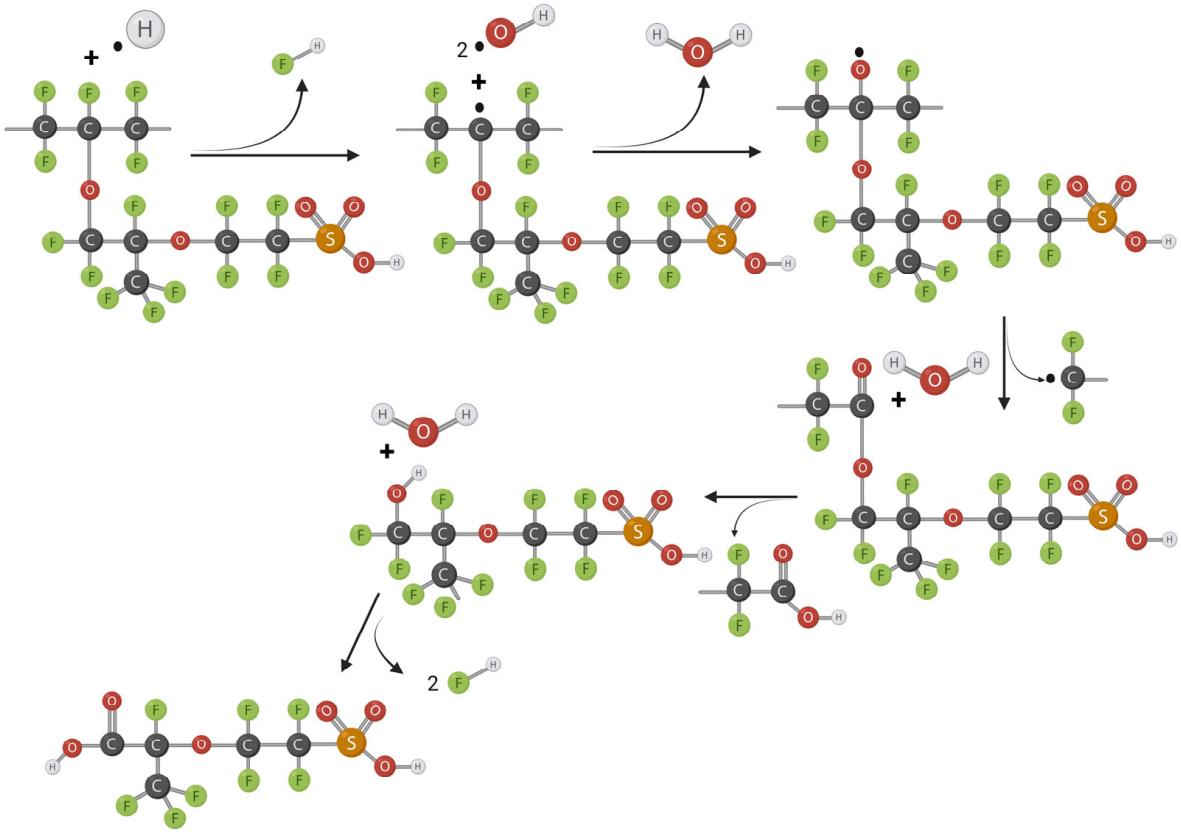

Figure 7. Main chain scission: radical attack to the tertiary backbone carbon bearing the side chain or the tertiary carbon between two ether groups within the side chain.

The ether group in the side chain has been proposed as another site for radical attack [77,78]. There are several possibilities through which the ether bond closer to the C-S bond, which is the preferred site for radical attack, can be cleaved (Figure 8). However, in all cases, the fragmented part ends up with a carboxylic acid end group, which would follow the unzipping mechanism, as explained above.

Conventionally, hydroxyl (•OH) or hydrogen atoms (•H) are considered the main radicals responsible for membrane degradation. Recent research has indicated the presence of hydronium radical (H_3O•), which can be produced by the reaction between •H and H_2O in PEMFCs [79]. The ab initio modeling suggested that H_3O• can be stabilized by the sulfonic anion on the polymer side chain. The polymer side chain can undergo a conformational change with the help of water, leading to a greatly reduced barrier for F extraction from the tertiary carbon (Figure 7), supporting the •H attack on the tertiary carbon mechanism.

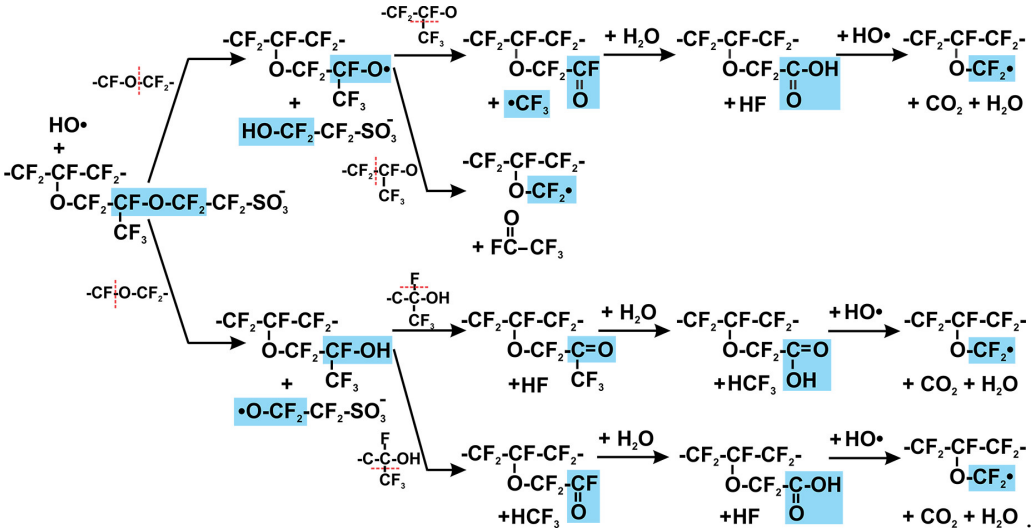

Figure 8. Side chain scission: radical attack on the C–O bond of the side chain. Reprinted with permission from [77].

All these radical attacks on the membrane cause a release of fluoride; different acids, including HF; and polymer fragments in the fuel cell system. The membrane resistance increases due to the loss of conducting functional groups. Weight, density, and water uptake properties are changed due to changes in the polymer backbone structure. Local or uniform membrane thinning causes severely reduced mechanical properties. Mostly, the formation of pinholes and cracks takes place, causing a high gas crossover rate, which is responsible for severe performance decay [80].

2.4. Mitigation Strategies

The main mitigation strategies to avoid chemical degradation are to avoid foreign impurities that can trigger radical formation and to improve the stability of membranes against radical attacks. To avoid the impurities that trigger unstable radical formation, especially the Fe^{2+} and Cu^{2+}, the materials of the bipolar plate can be modified. Composite bipolar plates could be one way to avoid such metal impurities coming from bipolar plate corrosion [81]. For the contamination coming through the air streams, several researchers have suggested using a more efficient air filter in the fuel cell system [43,82]. Filtering out NOx, sulfide, or other acidic substances from the air reduces the impact of gas impurities on fuel cell stack corrosion [83,84]. Several mitigation strategies, including on-site pre-treatment of reformation during hydrogen production, onboard CO removal, in operando CO mitigation, and the development of CO-tolerant catalysts, have been proposed to tackle the CO poisoning of the fuel cell [44,85]. Finally, to mitigate the radical attack on membranes, enhanced radical-tolerant membranes should be developed and commercialized [86]. Furthermore, some tuning of operating conditions can also be helpful in reducing membrane degradation. A moderate operating temperature, a lower hydrogen pressure, and a stable and uniform humidity distribution within the cell have been suggested to slow down membrane degradation rates [87].

3. Mechanical Degradation

The mechanical degradation of the membrane is caused by several factors, which are discussed next. Fuel cell testing over an extended period shows time-dependent deformation, such as micro-crack fractures appearing in the membrane. Such mechanical degradation results from cyclic stress applied to the membrane and strain from changes in the operating conditions. Relative humidity cycling, transients at open circuit voltage, temperature cycling, and potential cycling are among the most important factors causing mechanical defects in the membrane [88,89]. Some of these factors affect the mechanical

robustness of polymers more significantly than others; for instance, temperature cycling has been reported to have less influence on membrane breakdown than RH cycling.

3.1. Mechanical Stress

Localized mechanical stress caused by foreign particles, the gas diffusion layer's roughness, non-homogeneous conditions within the cell, and uneven clamping stress promote cracks and their expansion [90,91]. Moreover, the cyclic swelling and shrinking of the membrane reduce its strength, which finally leads to permanent plastic deformation, poor membrane–electrode interfacial contact, and micro defects [88]. Additionally, the active and non-active areas of the membrane expand to a different extent, causing mechanical stress at the corners [92]. Apart from the improper PEMFC manufacturing process, leaving particles, non-uniform clamping stress, and chemical degradation also make the membrane susceptible to mechanical degradation. Once the membrane is chemically degraded, its mechanical properties are reduced, and it becomes more vulnerable to the effects of changes in humidity, temperature, and pressure [93,94]. Moreover, the molecular weight of the membrane material can be significantly reduced by chemical degradation, causing the membrane to be brittle and accelerating the fracture and break due to uneven mechanical stress on the membrane [87].

3.2. Hygrothermal Cycling

The humidity of the membrane significantly affects its mechanical properties, such as strength and modulus. Hygrothermal cycling refers to the cyclic increase and decrease in temperature and humidity, especially during start-up procedures, that can influence the strength, modulus, and elongation at the break of the membrane. Kundu et al. [95] studied the mechanical properties of Nafion membranes under dry and hydrated conditions and found that membranes in a hydrated state exhibit reduced strength and modulus. Tang et al. [96] found that RH cycling of Nafion membranes from water-soaked state to 25% RH state caused cyclic stress up to 2.23 MPa with a dimensional change of ∼11%, while the safety limit of the cyclic stress for the particular Nafion membrane was only ∼1.5 MPa (Figure 9a).

3.3. Freeze–Thaw Cycling

The freeze–thaw cycle of the water confined in the MEA can lead to fuel cell performance loss and membrane degradation. The increased volume of ice in the enclosed MEA leads to the development of stress, causing microcrack growth and deformations [97]. McDonald et al. [98] studied the effects of freeze–thaw cycling on the chemical and physical properties of Nafion by subjecting it to 385 freeze–thaw cycles between +80 °C and −40 °C over a period of three months. The freeze–thaw cycling of membranes resulted in decreased strength and elongation at break.

3.4. Mitigation Strategies

To avoid mechanical degradation of membranes due to foreign particles, the gas diffusion layer's roughness and processing and manufacturing conditions should be improved. For example, Taylor et al. [99] suggested a calendering technique to flatten stray fibers within the gas diffusion media to mitigate pinhole formation in hot-pressed MEAs. Bipolar plate and cell design should be optimized to ensure uniform contact pressure. Excessive pressure cycling, overpressure, and pressure gradients should be avoided. The reinforcement of the membrane with, e.g., a porous polyethylene, PTFE, or oxides, enhances the dimensional stability and reduces the shrinkage stress in the membrane during drying [90,100]. Gas purging is among the thermal management strategies employed to control the temperature of water within the membrane during shutdown. Other approaches, such as heat preservation to prevent freezing and passive/active rapid startups from sub-zero environments, have also been explored [101]. Additionally, exposing the cell to dry gas (Figure 9b) or filling its components with an antifreeze solution have been proposed as

effective ways of averting ice accumulation in the MEA [102,103]. Furthermore, optimizing membrane humidity management involving avoiding air supply with supersaturated steam, minimizing humidity cycling, particularly at elevated humidification levels, and ensuring operating conditions that prevent membrane dry-out could limit membrane degradation [87].

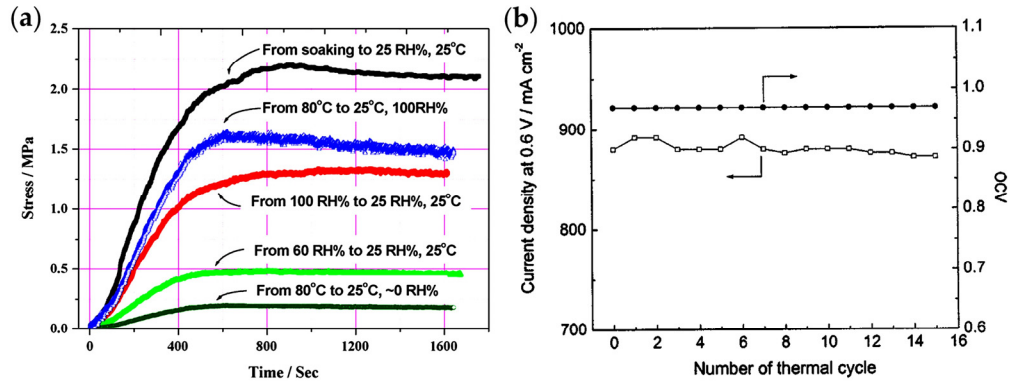

Figure 9. (**a**) Shrinkage stress of Nafion membrane at 25 °C at different humidities. (**b**) Effects of thermal cycle from 80 to −10 °C on the open-circuit voltage and current density after gas purging process. Adapted with permission (**a**) from [96] and (**b**) from [102].

4. Thermal Degradation

High-temperature operating conditions can increase the ion transport capacity of the membrane and promote the electrochemical reaction. However, if the temperature is excessively high (thermal stress), membrane failure can occur due to reduced water content (drying) and material degradation.

4.1. Thermal Stress and Cycling

The most favorable working temperature of a PEM fuel cell is usually from 60 to 80 °C to maintain the adequate hydration of the membrane. The conventional perfluorosulfonic acid membranes undergo serious breakdown at high temperatures because their glass transition temperature is around 80 °C [18]. Frensch et al. [104] found that the fluoride emission rate (Figure 10a) from Nafion and membrane thinning (Figure 10b) significantly increases at temperatures above 80 °C. Furthermore, hot spots or excess heat can severely accelerate membrane degradation. Current research mainly focuses on mechanical degradation and chemical degradation since PEMFCs are operated at lower temperatures. However, high-temperature operation can improve fuel cell performance by increasing the ion transport capacity of the membrane, enhancing the electrochemical reaction rate, and improving the water management system. Consequently, significant efforts have been made to develop PEM fuel cells that operate at a temperature of >100 °C. Nonetheless, the proton conductivity of PFSA membranes drops drastically when the fuel cell is operated at high temperatures due to reduced water content [105]. The mechanism of thermal degradation has not been sufficiently studied. The most widely accepted one is that high temperature leads to the decomposition of the side sulfonate acid group, which is similar to chemical degradation [106,107]; however, for such degradation, a considerably high temperature is required. In addition to high temperature, the subfreezing temperature (freeze–thaw cycling) causes membrane degradation, which has been discussed in Section 3.3.

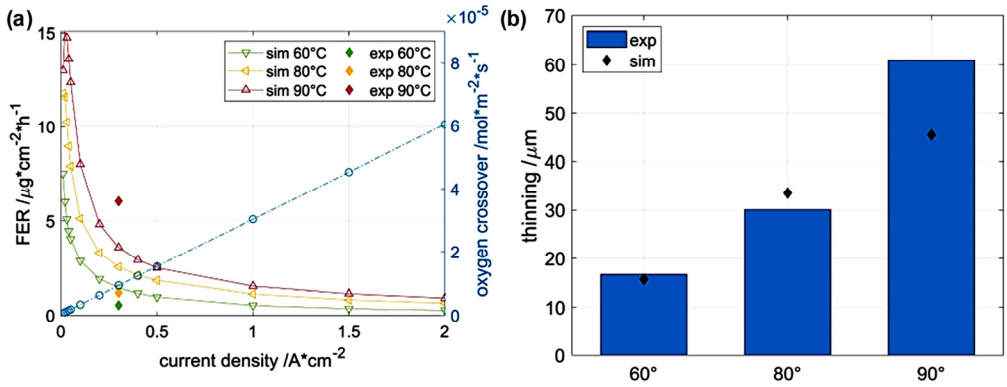

Figure 10. (**a**) The experimental and simulated fluoride emission rate (FER) from Nafion at different temperatures; experimental FER at 0.3 A cm^{-2} and simulated oxygen crossover from anode to cathode at 70 °C. (**b**) Membrane thinning determined by scanning electron microscope images and simulations. Adapted with permission from [104].

4.2. Drying

The drying of the membrane is related to high-temperature operation, which reduces the water content of the membrane. The proton conductivity of the membrane degrades significantly in dehydrated conditions at a high temperature and low humidity [105]. Furthermore, dry membranes are susceptible to crack formation, which critically affects their mechanical stability and promotes the formation of pinholes and gas crossover [108]. Apart from high-temperature operation, contaminant ions contribute to membrane drying and conductivity reduction [109,110]. Furthermore, long-term application may cause irreversible drying due to changes in the chemical nature of the membrane. Collette et al. [111] found that membrane degradation causes the alteration of sulfonic acid end groups when used over a period of 400 days. They discovered that the condensation of sulfonic acids produces sulfonic anhydride, leading to a considerable decrease in water uptake and thus the hydrophilicity of Nafion due to the substitution of ionic end groups with less hydrophilic anhydrides.

4.3. Mitigation Strategies

Thermal material degradation of membranes can be avoided by using moderate temperatures for operation, especially for PFSA membranes. The drying can be avoided by operating under proper humid conditions or using a humidifier. However, to operate the fuel cell at a higher temperature, membranes with better thermal stability and adequate conductivity under low humidity conditions should be developed. The thermal stability of membranes can be improved by using reinforcement or through modifications of the chemistry of the membrane materials. For example, a phosphoric acid-doped polybenzimidazole membrane has been developed to achieve higher thermal stability [112]. Furthermore, nanocomposite membranes with several fillers, such as SiO_2, mordenite, zirconia, TiO_2, and graphene oxide, have been explored to improve mechanical and thermal stability [113]. Degradation due to hot spots or excess heat can be avoided by proper heat management and water management and their combined optimization [114–117].

5. Progress in PEM Development for Fuel Cells

The advances in PEM fuel cell membrane development target improving thermal stability for high-temperature applications, along with enhanced conductivity and mechanical properties [118–120]. The approaches can be divided into (i) modifications in the chemistry of membrane materials and (ii) developing composite membranes.

5.1. Chemically Modified PEMs

Several attempts have been made to modify the structure of Nafion to achieve advantageous properties. The research has led to several commercial membranes, such as Aquivion®, Hyflon®, Flemion®, and Dyneon$_{TM}$, based on shorter side sulfonic chains compared with Nafion [119]. Furthermore, the whole range of new materials has been tested as proton exchange membranes for high-temperature fuel cell applications. Several sulfonated polymers, such as polyether ketones, polyphenylsulfone, and poly(arylene ether), have been widely studied as PEMs due to their good stability at high temperatures and low cost [121–126]. However, sulfonated polyether ketone membranes, like the PFSA membranes, undergo degradation due to dehydration under high operating temperatures. Polybenzimidazole (PBI) is an aromatic linear heterocyclic rigid semi-crystalline polymer containing repeated benzimidazole units with excellent chemical resistance, high mechanical strength, good moisture regain, and thermo-oxidative stability above 80 °C [127]. PBI and acid-doped PBI-based membranes have been considered for high-temperature applications because of their excellent chemical and thermal properties at elevated temperatures without the need for humidification and their low cost [11,113]. Different acids, such as HNO_3, H_2SO_4, HCl, and $HClO_4$, can be doped into PBI membranes to act as proton donors. However, phosphoric acid (H_3PO_4) has been a favored dopant because compared with others, it induces higher conductivity and excellent thermal stability in PBI membranes without the need for high RH [128,129]. Jin et al. [130] developed poly(arylene pyridine) using one-step Friedel–Crafts polymerization of 4-acetylpyridine and para-terphenyl/biphenyl; the resulting membrane from the polymer exhibited excellent phosphoric acid uptake (up to 220%) with a conductivity of 0.102 S cm^{-1} at 180 °C. Hu et al. [131] fabricated a phosphoric acid-doped triazole-functionalized poly(arylene perfluorophenyl)-based membrane with similar conductivity at 180 °C (0.109 S cm^{-1}), whereas Li et al. [132] synthesized poly(terphenyl pyridine) polymers using 4-acetylpyridine, p-terphenyl, and comonomer 2,2,2-trifluoroacetophenone via the acid-catalyzed polycondensation reaction. The prepared membranes using the synthesized polymer doped with phosphoric acid exhibited a proton conductivity of 0.142 S cm^{-1} at 160 °C under anhydrous conditions and a peak power density of 395 mW cm^{-2} at 180 °C in a single fuel cell fueled by non-humidified H_2 and O_2. The major issues with the H_3PO_4-doped PBI membranes are catalyst poisoning and other types of fuel cell component degradation due to acid leaching and undesirable electrochemical reactions. Another chemically different membrane is an acid–base membrane in which a non-aqueous solvent, like acid or protic ionic liquid, replaces water and acts as a proton carrier while a solid material provides the medium for proton conduction. The proton-conducting medium is mostly based on polymers with basic moieties, such as amine, amide, imide, alcohol, ether, or aprotic ionic liquid, which can react with acid to form a complex acid–base polymer membrane with proton conductivity (such as acid-doped PBI). For example, Huang et al. [133] incorporated hindered amine and imidazole in the PFSA membranes, forming an acid–base crosslinking and interpenetrating network structure for continuous proton transport and providing membranes with excellent dimensional stability and radical scavenging properties. An increase in the proton carrier acid content of the membrane can improve the proton conductivity but leads to poor mechanical stability, especially at temperatures greater than 100 °C [113].

In addition to improving the mechanical and thermal stability, the chemical modification of the membrane to incorporate radical scavenging properties has also been attempted. Wang et al. [134] grafted organic free radical scavengers, such as 2-mercapto-1-methylimidazole, 3-mercapto-1,2,4-triazole, and 2-mercaptobenzimidazole into the polyarylethersulfone backbone. Around 200 wt% phosphoric acid-doped 2-mercapto-1-methylimidazole-grafted polyarylethersulfone membranes exhibited an anhydrous proton conductivity of 78.3 mS cm^{-1} at 180 °C, a tensile strength of 7.8 MPa at room temperature, and a peak power density of 423 mW cm^{-2} at 160 °C with a fuel cell fueled by non-humidified H_2 and O_2. Agarwal et al. [135] incorporated phosphonic acid into Nafion membranes as a radical scavenger and compared the performance with membranes incor-

porated with widely the reported radical scavenger cerium. The fluoride emission rates of phosphonic acid-Nafion membranes were much lower than the baseline (non-modified Nafion) and cerium-incorporated Nafion (Ce), especially for the phosphonic acid with the shortest perfluoro chains (C6) (Figure 11a). The ratio of fluorescence intensity (I) after the addition of Fenton's reagent with and without scavengers to the fluorescence intensity of the undegraded dye (I_0) exhibited higher retention of the intensity of the fluorescent dye (I) for phosphonic acid–Nafion compared to cerium–Nafion, indicating that phosphonic acid has a higher radical scavenging capability (Figure 11b). Even the conductivity (although not surprising given that phosphonic acids are proton conductors) and water uptake of phosphonic acid–Nafion increased (Figure 11c,d). However, the strength of the phosphonic acid–Nafion decreased from baseline, while the strength of cerium–Nafion increased from baseline, although this made it more brittle, with a higher modulus and a lower elongation at break (Figure 11e). Moreover, the Nafion membrane itself has been chemically modified to improve the radical tolerance and proton conductivity. Teixeira et al. [136] doped Nafion membranes with bisphosphonic acids and found that the doped membranes have better chemical stability after oxidative degradation under Fenton's test conditions at 80 °C.

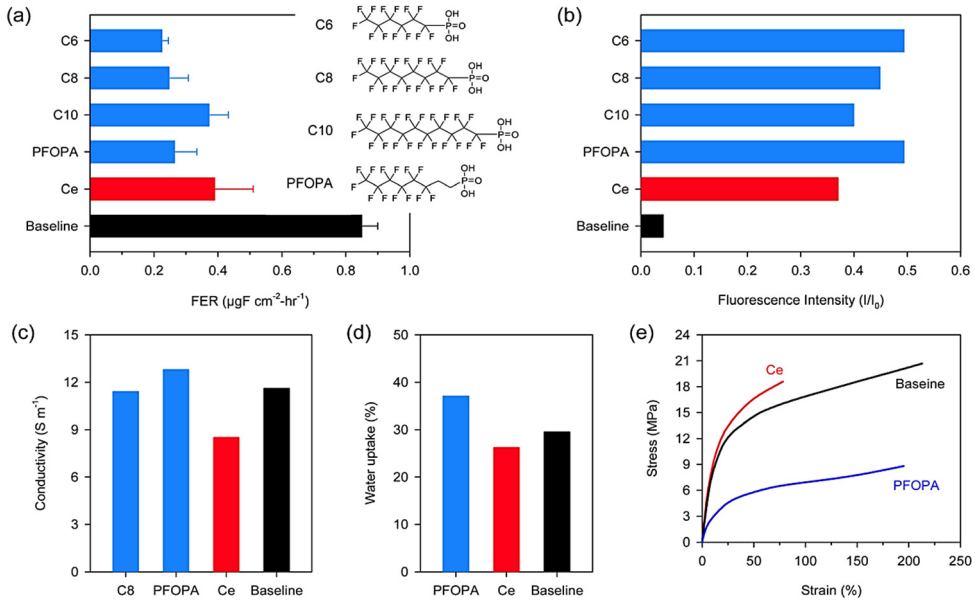

Figure 11. Various properties of radical scavenger-incorporated Nafion membranes: (**a**) fluoride emission rate over 24 h of aqueous Fenton test, (**b**) retention of 6-carboxyfluorescein intensity in the presence of different radical scavengers, (**c**) proton conductivity at 80 °C and 100% RH, (**d**) water update at room temperature, and (**e**) stress–strain curves under ambient conditions. Reprinted from [135].

5.2. Composite PEMs

The sulfonic acid groups of PFSA membranes can undergo dynamic cross-linking with hygroscopic inorganic materials, like Al_2O_3, TiO_2, SiO_2, ZrO_2, mordenite, graphene oxide, ionic liquids, and layered double hydroxide nanoparticles [113]. The dispersion of these particles in the polymer matrix enhances water retention and porosity while reducing gas crossover in the membrane [15,137]. However, incorporating hydrophilic inorganic additives into conducting membranes generally decreases proton conductivity due to the insulation effects of fillers. Numerous strategies have been employed to improve conductivity, including (i) functionalizing inorganic additives, (ii) integrating inorganic binary component materials, and (iii) introducing proton-conductive fillers [138]. Each type of inorganic particle provides specific benefits to membranes; for example, silica particles and ZrO_2 reduce membrane swelling, increase water uptake, and improve proton conductivity [139–141]. TiO_2 reduces methanol crossover, improves mechanical and

thermal properties, and increases water absorption [142,143]. However, the low compatibility between polymers and fillers may impact the physical and mechanical properties of the membranes [144]. Carbon-based nanomaterials, such as carbon nanotubes [145], graphene [146], fullerenes [147], and nanodiamond [148] are promising reinforcements for improving the performance of PEM. Metal–organic frameworks (MOFs) are crystalline porous materials with three-dimensional network structures formed by organic–inorganic self-assembly [15,149]. MOFs have been extensively investigated as fillers in PEMs due to their ability to be tuned for target applications. MOFs can improve the water retention ability and proton conductivity of PFSA membranes [150]. Ionic liquids (ILs) are molten salts in the liquid state at room temperature, typically defined as liquid electrolytes composed entirely of ions without the use of solvents. Some ILs have excellent ionic conductivities even under anhydrous conditions and are, therefore, widely studied as reinforcement in membranes for PEMFC applications [151,152]. Polymeric reinforcement is another technique that has been investigated for developing composite PEMs [143]. Several polymers, such as polytetrafluoroethylene, polyvinylidene fluoride, and polybenzimidazole, have been incorporated into PSFA membranes to improve their performance [138,143].

Several nanomaterials with radical scavenging properties have been incorporated into membranes to improve radical tolerance, with cerium-based materials being the most popular [153–155]. Tinh et al. [156] used cerium oxide particles (5–7 nm) produced by the sol-gel method to fabricate durable layered membranes containing cerium oxide spheres on both surface layers. The smaller particles did not affect the proton conductivity of the membrane while providing radical scavenging effects. Cerium is widely used and is an effective radical scavenger; however, the migration of cerium ions to the catalyst layer during fuel cell operation causes a loss in durability and performance due to adverse effects on various components of the fuel cell. Xu et al. [157] co-doped organic antioxidant alizarin and cerium ions to fabricate PFSA composite membranes with improved oxidative stability and the reduced migration of cerium ions from the membrane. Agarwal et al. [158] used 15-Crown-5 to immobilize cerium within PFSA membranes by forming an organometallic complex of cerium with 15-Crown-5. Another way of encapsulating free radical scavengers could be fabricating a thin conductive layer on the CeO_x-containing membranes [159]. Zhiyan et al. [160] changed the morphology of ceria from conventional nanoparticles to nanorods, significantly reducing the migration of cerium. Moreover, ferrocyanide, ferricyanide, and MnO_x are among other radical scavenging materials being used to fabricate composite PEMs [161–163].

6. Conclusions and Outlook

Proton exchange membrane fuel cells have the potential to tackle major challenges associated with fossil fuel-sourced energy consumption and accompanying environmental complications. However, PEM degradation is one of the significant issues in the operation of PEMFCs in the long term or at subfreezing and elevated temperatures. There are several routes of membrane degradation, which can be divided into chemical, mechanical, and thermal degradation. We have reviewed different pathways of PFSA degradation, the underlying mechanisms, and the mitigation strategies. The chemical degradation of the membrane caused by radical attack, which is accelerated by the presence of metal impurities such as Fe^{2+} and Cu^{2+}, is the most severe threat, which can be avoided by using composite bipolar plates. There are several advantages of composite bipolar plates, such as their light weight, high corrosion resistance, and stability under harsh conditions; however, it has been difficult for composite materials to satisfy the electrical conductivity requirements due to the poor intrinsic electrical properties of polymers [81]. Therefore, extensive research is needed to develop high-performance, advantageous composite bipolar plates. The mechanical degradation of membranes is mostly caused by non-uniform conditions, cyclic humidity change, and cyclic thermal stress, and these triggers can be avoided by membrane modification, better manufacturing practices, and optimized operating conditions. The research should be focused on fabricating robust membranes and optimizing the thermal,

water, and gas management in the fuel cell system. Furthermore, the use of conventional PFSA membranes such as PEM shows limitations in terms of low proton conductivity in anhydrous conditions and degradation in mechanical and physical properties at elevated temperatures. Consequently, several advances in the manufacturing of PEMs have been made to develop membranes that could be used under high-temperature and low-humidity conditions and that are tolerant to impurities and radical attacks. However, these membranes still have some limitations, such as the leaching of acid or metal ions from fillers. Recently, many advancements have been made, especially in membranes incorporated with radical scavengers. Nevertheless, most of these membranes have yet to reach the level of commercial applications that PFSA membranes have reached. Therefore, producing robust fuel cell membranes tolerant to diverse operating conditions, impurities, and radical attacks at the commercial level is still a fruitful direction of research and will boost the widespread application of fuel cells in diverse conditions.

Author Contributions: Conceptualization, methodology, D.M. and V.V.; investigation, formal analysis, D.M.; visualization, D.M., J.W. and R.K.; writing—original draft preparation, D.M.; writing—review and editing, D.M., J.W., R.K., J.M., F.B. and V.V. All authors have read and agreed to the published version of the manuscript.

Funding: This research was funded by Fonds Wetenschappelijk Onderzoek—Vlaanderen (FWO) strategic basic research fellowships (grant numbers: 1S13922N and 1SHI624N).

Data Availability Statement: The study did not produce any data.

Acknowledgments: D.M. and J.W. acknowledge support from Fonds Wetenschappelijk Onderzoek —Vlaanderen (FWO) for their strategic basic research fellowships.

Conflicts of Interest: The authors declare no conflicts of interest. The funders had no role in the design of the study; in the collection, analyses, or interpretation of data; in the writing of the manuscript; or in the decision to publish the results.

References

1. Stančin, H.; Mikulčić, H.; Wang, X.; Duić, N. A Review on Alternative Fuels in Future Energy System. *Renew. Sustain. Energy Rev.* **2020**, *128*, 109927. [CrossRef]
2. Halkos, G.E.; Gkampoura, E.-C. Reviewing Usage, Potentials, and Limitations of Renewable Energy Sources. *Energies* **2020**, *13*, 2906. [CrossRef]
3. Madhav, D.; Buffel, B.; Desplentere, F.; Moldenaers, P.; Vandeginste, V. Bio-Inspired Mineralization of CO_2 into $CaCO_3$: Single-Step Carbon Capture and Utilization with Controlled Crystallization. *Fuel* **2023**, *345*, 128157. [CrossRef]
4. Madhav, D.; Coppitters, T.; Ji, Y.; Thielemans, W.; Desplentere, F.; Moldenaers, P.; Vandeginste, V. Amino Acid Promoted Single-Step Carbon Dioxide Capture and Mineralization Integrated with Polymer-Mediated Crystallization of Carbonates. *J. Clean. Prod.* **2023**, *415*, 137845. [CrossRef]
5. Madhav, D.; Chergaoui, S.; Vandeginste, V. Carbon Capture by Amino Acid Materials. In *Reference Module in Earth Systems and Environmental Sciences*; Elsevier: Amsterdam, The Netherlands, 2023; ISBN 978-0-12-409548-9.
6. Winter, M.; Brodd, R.J. What Are Batteries, Fuel Cells, and Supercapacitors? *Chem. Rev.* **2004**, *104*, 4245–4270. [CrossRef]
7. Yatoo, M.A.; Habib, F.; Malik, A.H.; Qazi, M.J.; Ahmad, S.; Ganayee, M.A.; Ahmad, Z. Solid-Oxide Fuel Cells: A Critical Review of Materials for Cell Components. *MRS Commun.* **2023**, *13*, 378–384. [CrossRef]
8. Borup, R.; Meyers, J.; Pivovar, B.; Kim, Y.S.; Mukundan, R.; Garland, N.; Myers, D.; Wilson, M.; Garzon, F.; Wood, D.; et al. Scientific Aspects of Polymer Electrolyte Fuel Cell Durability and Degradation. *Chem. Rev.* **2007**, *107*, 3904–3951. [CrossRef] [PubMed]
9. Shabani, B.; Andrews, J. Hydrogen and Fuel Cells. In *Energy Sustainability Through Green Energy*; Sharma, A., Kar, S.K., Eds.; Green Energy and Technology; Springer: New Delhi, India, 2015; pp. 453–491. ISBN 978-81-322-2337-5.
10. Xing, Y.; Li, H.; Avgouropoulos, G. Research Progress of Proton Exchange Membrane Failure and Mitigation Strategies. *Materials* **2021**, *14*, 2591. [CrossRef] [PubMed]
11. Li, Q.; Jensen, J.O.; Savinell, R.F.; Bjerrum, N.J. High Temperature Proton Exchange Membranes Based on Polybenzimidazoles for Fuel Cells. *Prog. Polym. Sci.* **2009**, *34*, 449–477. [CrossRef]
12. Souzy, R.; Ameduri, B. Functional Fluoropolymers for Fuel Cell Membranes. *Prog. Polym. Sci.* **2005**, *30*, 644–687. [CrossRef]
13. Miyake, J.; Miyatake, K. Fluorine-Free Sulfonated Aromatic Polymers as Proton Exchange Membranes. *Polym. J.* **2017**, *49*, 487–495. [CrossRef]
14. Adamski, M.; Peressin, N.; Holdcroft, S. On the Evolution of Sulfonated Polyphenylenes as Proton Exchange Membranes for Fuel Cells. *Mater. Adv.* **2021**, *2*, 4966–5005. [CrossRef]

15. Zhu, L.-Y.; Li, Y.-C.; Liu, J.; He, J.; Wang, L.-Y.; Lei, J.-D. Recent Developments in High-Performance Nafion Membranes for Hydrogen Fuel Cells Applications. *Pet. Sci.* **2022**, *19*, 1371–1381. [CrossRef]
16. Peighambardoust, S.J.; Rowshanzamir, S.; Amjadi, M. Review of the Proton Exchange Membranes for Fuel Cell Applications. *Int. J. Hydrogen Energy* **2010**, *35*, 9349–9384. [CrossRef]
17. Schiraldi, D.A. Perfluorinated Polymer Electrolyte Membrane Durability. *J. Macromol. Sci. Part C* **2006**, *46*, 315–327. [CrossRef]
18. Zhang, J.; Zhang, H.; Wu, J.; Zhang, J. Chapter 11—Fuel Cell Degradation and Failure Analysis. In *Pem Fuel Cell Testing and Diagnosis*; Zhang, J., Zhang, H., Wu, J., Zhang, J., Eds.; Elsevier: Amsterdam, The Netherlands, 2013; pp. 283–335. ISBN 978-0-444-53688-4.
19. Yuan, X.-Z.; Nayoze-Coynel, C.; Shaigan, N.; Fisher, D.; Zhao, N.; Zamel, N.; Gazdzicki, P.; Ulsh, M.; Friedrich, K.A.; Girard, F.; et al. A Review of Functions, Attributes, Properties and Measurements for the Quality Control of Proton Exchange Membrane Fuel Cell Components. *J. Power Sources* **2021**, *491*, 229540. [CrossRef]
20. Okada, T.; Møller-Holst, S.; Gorseth, O.; Kjelstrup, S. Transport and Equilibrium Properties of Nafion® Membranes with H^+ and Na^+ Ions. *J. Electroanal. Chem.* **1998**, *442*, 137–145. [CrossRef]
21. Kelly, M.J.; Fafilek, G.; Besenhard, J.O.; Kronberger, H.; Nauer, G.E. Contaminant Absorption and Conductivity in Polymer Electrolyte Membranes. *J. Power Sources* **2005**, *145*, 249–252. [CrossRef]
22. Holladay, J.D.; Hu, J.; King, D.L.; Wang, Y. An Overview of Hydrogen Production Technologies. *Catal. Today* **2009**, *139*, 244–260. [CrossRef]
23. Zhao, Y.; Mao, Y.; Zhang, W.; Tang, Y.; Wang, P. Reviews on the Effects of Contaminations and Research Methodologies for PEMFC. *Int. J. Hydrogen Energy* **2020**, *45*, 23174–23200. [CrossRef]
24. Madhav, D.; Shao, C.; Mus, J.; Buysschaert, F.; Vandeginste, V. The Effect of Salty Environments on the Degradation Behavior and Mechanical Properties of Nafion Membranes. *Energies* **2023**, *16*, 2256. [CrossRef]
25. Gao, G.; Wang, S.; Xue, R.; Liu, D.; Ren, H.; Zhang, R. Uncovering the Characteristics of Air Pollutants Emission in Industrial Parks and Analyzing Emission Reduction Potential: Case Studies in Henan, China. *Sci. Rep.* **2021**, *11*, 23709. [CrossRef] [PubMed]
26. Cheng, X.; Shi, Z.; Glass, N.; Zhang, L.; Zhang, J.; Song, D.; Liu, Z.-S.; Wang, H.; Shen, J. A Review of PEM Hydrogen Fuel Cell Contamination: Impacts, Mechanisms, and Mitigation. *J. Power Sources* **2007**, *165*, 739–756. [CrossRef]
27. Novalin, T.; Eriksson, B.; Proch, S.; Bexell, U.; Moffatt, C.; Westlinder, J.; Lagergren, C.; Lindbergh, G.; Lindström, R.W. Trace-Metal Contamination in Proton Exchange Membrane Fuel Cells Caused by Laser-Cutting Stains on Carbon-Coated Metallic Bipolar Plates. *Int. J. Hydrogen Energy* **2021**, *46*, 13855–13864. [CrossRef]
28. Li, H.; Tsay, K.; Wang, H.; Shen, J.; Wu, S.; Zhang, J.; Jia, N.; Wessel, S.; Abouatallah, R.; Joos, N.; et al. Durability of PEM Fuel Cell Cathode in the Presence of Fe^{3+} and Al^{3+}. *J. Power Sources* **2010**, *195*, 8089–8093. [CrossRef]
29. Sulek, M.; Adams, J.; Kaberline, S.; Ricketts, M.; Waldecker, J.R. In Situ Metal Ion Contamination and the Effects on Proton Exchange Membrane Fuel Cell Performance. *J. Power Sources* **2011**, *196*, 8967–8972. [CrossRef]
30. Wang, X.; Qi, J.; Ozdemir, O.; Uddin, A.; Pasaogullari, U.; Bonville, L.J.; Molter, T. Ca^{2+} as an Air Impurity in Polymer Electrolyte Membrane Fuel Cells. *J. Electrochem. Soc.* **2014**, *161*, F1006. [CrossRef]
31. Uddin, M.A.; Wang, X.; Park, J.; Pasaogullari, U.; Bonville, L. Distributed Effects of Calcium Ion Contaminant on Polymer Electrolyte Fuel Cell Performance. *J. Power Sources* **2015**, *296*, 64–69. [CrossRef]
32. Qi, J.; Ge, J.; Uddin, M.A.; Zhai, Y.; Pasaogullari, U.; St-Pierre, J. Evaluation of Cathode Contamination with Ca2+ in Proton Exchange Membrane Fuel Cells. *Electrochim. Acta* **2018**, *259*, 510–516. [CrossRef]
33. Zhu, J.; Tan, J.; Pan, Q.; Liu, Z.; Hou, Q. Effects of Mg^{2+} Contamination on the Performance of Proton Exchange Membrane Fuel Cell. *Energy* **2019**, *189*, 116135. [CrossRef]
34. Li, G.; Tan, J.; Gong, J.; Zhang, X.; Xin, Y.; Hu, X. Performance of Proton Exchange Membrane in the Presence of Mg^{2+}. *J. Fuel Cell Sci. Technol.* **2014**, *11*, 044501. [CrossRef]
35. Qi, J.; Wang, X.; Ozdemir, M.O.; Uddin, M.A.; Bonville, L.; Pasaogullari, U.; Molter, T. Effect of Cationic Contaminants on Polymer Electrolyte Fuel Cell Performance. *J. Power Sources* **2015**, *286*, 18–24. [CrossRef]
36. Hongsirikarn, K.; Goodwin, J.G.; Greenway, S.; Creager, S. Effect of Cations (Na^+, Ca^{2+}, Fe^{3+}) on the Conductivity of a Nafion Membrane. *J. Power Sources* **2010**, *195*, 7213–7220. [CrossRef]
37. Okada, T.; Satou, H.; Okuno, M.; Yuasa, M. Ion and Water Transport Characteristics of Perfluorosulfonated Ionomer Membranes with H+ and Alkali Metal Cations. *J. Phys. Chem. B* **2002**, *106*, 1267–1273. [CrossRef]
38. Lee, C.; Wang, X.; Peng, J.-K.; Katzenberg, A.; Ahluwalia, R.K.; Kusoglu, A.; Komini Babu, S.; Spendelow, J.S.; Mukundan, R.; Borup, R.L. Toward a Comprehensive Understanding of Cation Effects in Proton Exchange Membrane Fuel Cells. *ACS Appl. Mater. Interfaces* **2022**, *14*, 35555–35568. [CrossRef]
39. Li, H.; You, J.; Cheng, X.; Yan, X.; Shen, S.; Zhang, J. New Insight into the Effect of Co^{2+} Contamination on Local Oxygen Transport in PEMFCs. *Chem. Eng. J.* **2023**, *453*, 139945. [CrossRef]
40. Kienitz, B.L.; Baskaran, H.; Zawodzinski, T.A. Modeling the Steady-State Effects of Cationic Contamination on Polymer Electrolyte Membranes. *Electrochim. Acta* **2009**, *54*, 1671–1679. [CrossRef]
41. Zhu, F.; Wu, A.; Luo, L.; Wang, C.; Yang, F.; Wei, G.; Xia, G.; Yin, J.; Zhang, J. The Asymmetric Effects of Cu^{2+} Contamination in a Proton Exchange Membrane Fuel Cell (PEMFC). *Fuel Cells* **2020**, *20*, 196–202. [CrossRef]

42. Zhang, G.; Yang, G.; Shen, Q.; Li, S.; Li, Z.; Liao, J.; Jiang, Z.; Wang, H.; Zhang, H.; Ye, W. Study on the Transport Performance Degradation of Nafion Membrane Due to the Presence of Na^+ and Ca^{2+} Using Molecular Dynamics Simulations. *J. Power Sources* **2022**, *542*, 231740. [CrossRef]
43. Xie, M.; Zhang, Q.; Yang, D.; Chu, T.; Li, B.; Ming, P.; Zhang, C. The Synergetic Effect of Air Pollutants and Metal Ions on Performance of a 5 kW Proton-Exchange Membrane Fuel Cell Stack. *Int. J. Energy Res.* **2021**, *45*, 7974–7986. [CrossRef]
44. Valdés-López, V.F.; Mason, T.; Shearing, P.R.; Brett, D.J.L. Carbon Monoxide Poisoning and Mitigation Strategies for Polymer Electrolyte Membrane Fuel Cells—A Review. *Prog. Energy Combust. Sci.* **2020**, *79*, 100842. [CrossRef]
45. Baschuk, J.J.; Li, X. Carbon Monoxide Poisoning of Proton Exchange Membrane Fuel Cells. *Int. J. Energy Res.* **2001**, *25*, 695–713. [CrossRef]
46. Sethuraman, V.A.; Weidner, J.W. Analysis of Sulfur Poisoning on a PEM Fuel Cell Electrode. *Electrochim. Acta* **2010**, *55*, 5683–5694. [CrossRef]
47. Gomez, Y.A.; Oyarce, A.; Lindbergh, G.; Lagergren, C. Ammonia Contamination of a Proton Exchange Membrane Fuel Cell. *J. Electrochem. Soc.* **2018**, *165*, F189. [CrossRef]
48. Zhang, X.; Pasaogullari, U.; Molter, T. Influence of Ammonia on Membrane-Electrode Assemblies in Polymer Electrolyte Fuel Cells. *Int. J. Hydrogen Energy* **2009**, *34*, 9188–9194. [CrossRef]
49. Uribe, F.A.; Gottesfeld, S.; Zawodzinski, T.A. Effect of Ammonia as Potential Fuel Impurity on Proton Exchange Membrane Fuel Cell Performance. *J. Electrochem. Soc.* **2002**, *149*, A293. [CrossRef]
50. Narusawa, K.; Hayashida, M.; Kamiya, Y.; Roppongi, H.; Kurashima, D.; Wakabayashi, K. Deterioration in Fuel Cell Performance Resulting from Hydrogen Fuel Containing Impurities: Poisoning Effects by CO, CH_4, HCHO and HCOOH. *JSAE Rev.* **2003**, *24*, 41–46. [CrossRef]
51. Nachiappan, N.; Kalaignan, G.P.; Sasikumar, G. Influence of Methanol Impurity in Hydrogen on PEMFC Performance. *Ionics* **2013**, *19*, 517–522. [CrossRef]
52. Wang, X.; Baker, P.; Zhang, X.; Garces, H.F.; Bonville, L.J.; Pasaogullari, U.; Molter, T.M. An Experimental Overview of the Effects of Hydrogen Impurities on Polymer Electrolyte Membrane Fuel Cell Performance. *Int. J. Hydrogen Energy* **2014**, *39*, 19701–19713. [CrossRef]
53. Shabani, B.; Hafttananian, M.; Khamani, S.; Ramiar, A.; Ranjbar, A.A. Poisoning of Proton Exchange Membrane Fuel Cells by Contaminants and Impurities: Review of Mechanisms, Effects, and Mitigation Strategies. *J. Power Sources* **2019**, *427*, 21–48. [CrossRef]
54. Talke, A.; Misz, U.; Konrad, G.; Heinzel, A. Impact of Air Contaminants on Subscale Single Fuel Cells and an Automotive Short Stack. *JEE* **2015**, *3*, 70–79. [CrossRef]
55. Lemaire, O.; Barthe, B.; Rouillon, L.; Franco, A.A. Mechanistic Investigations of NO_2 Impact on ORR in PEM Fuel Cells: A Coupled Experimental and Multi-Scale Modeling Approach. *ECS Trans.* **2009**, *25*, 1595. [CrossRef]
56. Misz, U.; Talke, A.; Heinzel, A.; Konrad, G. Sensitivity Analyses on the Impact of Air Contaminants on Automotive Fuel Cells. *Fuel Cells* **2016**, *16*, 444–462. [CrossRef]
57. Talke, A.; Misz, U.; Konrad, G.; Heinzel, A.; Klemp, D.; Wegener, R. Influence of Urban Air on Proton Exchange Membrane Fuel Cell Vehicles—Long Term Effects of Air Contaminants in an Authentic Driving Cycle. *J. Power Sources* **2018**, *400*, 556–565. [CrossRef]
58. Hongsirikarn, K.; Goodwin, J.G.; Greenway, S.; Creager, S. Influence of Ammonia on the Conductivity of Nafion Membranes. *J. Power Sources* **2010**, *195*, 30–38. [CrossRef]
59. Doyle, M.; Lewittes, M.E.; Roelofs, M.G.; Perusich, S.A.; Lowrey, R.E. Relationship between Ionic Conductivity of Perfluorinated Ionomeric Membranes and Nonaqueous Solvent Properties. *J. Membr. Sci.* **2001**, *184*, 257–273. [CrossRef]
60. Zhou, Y.; Lu, C.; Cheng, J.; Xu, W.; Sun, Y.; Li, H.; Xu, L. Development of Hydrogen Fuel Cell Technology and Prospect for Its Military Application. In Proceedings of the Communications, Signal Processing, and Systems, Changbaishan, China, 24–25 July 2021; Liang, Q., Wang, W., Liu, X., Na, Z., Li, X., Zhang, B., Eds.; Springer: Singapore, 2021; pp. 1722–1730.
61. Moore, J.M.; Adcock, P.L.; Lakeman, J.B.; Mepsted, G.O. The Effects of Battlefield Contaminants on PEMFC Performance. *J. Power Sources* **2000**, *85*, 254–260. [CrossRef]
62. Okonkwo, P.C.; Ben Belgacem, I.; Emori, W.; Uzoma, P.C. Nafion Degradation Mechanisms in Proton Exchange Membrane Fuel Cell (PEMFC) System: A Review. *Int. J. Hydrogen Energy* **2021**, *46*, 27956–27973. [CrossRef]
63. Robert, M.; El Kaddouri, A.; Perrin, J.-C.; Mozet, K.; Daoudi, M.; Dillet, J.; Morel, J.-Y.; André, S.; Lottin, O. Effects of Conjoint Mechanical and Chemical Stress on Perfluorosulfonic-Acid Membranes for Fuel Cells. *J. Power Sources* **2020**, *476*, 228662. [CrossRef]
64. Fang, X.; Shen, P.K.; Song, S.; Stergiopoulos, V.; Tsiakaras, P. Degradation of Perfluorinated Sulfonic Acid Films: An in-Situ Infrared Spectro-Electrochemical Study. *Polym. Degrad. Stab.* **2009**, *94*, 1707–1713. [CrossRef]
65. Gubler, L.; Dockheer, S.M.; Koppenol, W.H. Radical (HO•, H• and HOO•) Formation and Ionomer Degradation in Polymer Electrolyte Fuel Cells. *J. Electrochem. Soc.* **2011**, *158*, B755. [CrossRef]
66. Zhao, M.; Shi, W.; Wu, B.; Liu, W.; Liu, J.; Xing, D.; Yao, Y.; Hou, Z.; Ming, P.; Zou, Z. Influence of Membrane Thickness on Membrane Degradation and Platinum Agglomeration under Long-Term Open Circuit Voltage Conditions. *Electrochim. Acta* **2015**, *153*, 254–262. [CrossRef]

67. Frühwirt, P.; Kregar, A.; Törring, J.T.; Katrašnik, T.; Gescheidt, G. Holistic Approach to Chemical Degradation of Nafion Membranes in Fuel Cells: Modelling and Predictions. *Phys. Chem. Chem. Phys.* **2020**, *22*, 5647–5666. [CrossRef] [PubMed]
68. Shah, A.A.; Ralph, T.R.; Walsh, F.C. Modeling and Simulation of the Degradation of Perfluorinated Ion-Exchange Membranes in PEM Fuel Cells. *J. Electrochem. Soc.* **2009**, *156*, B465. [CrossRef]
69. Curtin, D.E.; Lousenberg, R.D.; Henry, T.J.; Tangeman, P.C.; Tisack, M.E. Advanced Materials for Improved PEMFC Performance and Life. *J. Power Sources* **2004**, *131*, 41–48. [CrossRef]
70. Chen, C.; Fuller, T.F. The Effect of Humidity on the Degradation of Nafion® Membrane. *Polym. Degrad. Stab.* **2009**, *94*, 1436–1447. [CrossRef]
71. Xie, T.; Hayden, C.A. A Kinetic Model for the Chemical Degradation of Perfluorinated Sulfonic Acid Ionomers: Weak End Groups versus Side Chain Cleavage. *Polymer* **2007**, *48*, 5497–5506. [CrossRef]
72. Robert, M.; El Kaddouri, A.; Perrin, J.-C.; Raya, J.; Lottin, O. Time-Resolved Monitoring of Composite Nafion™ XL Membrane Degradation Induced by Fenton's Reaction. *J. Membr. Sci.* **2021**, *621*, 118977. [CrossRef]
73. Mittal, V.O.; Kunz, H.R.; Fenton, J.M. Membrane Degradation Mechanisms in PEMFCs. *J. Electrochem. Soc.* **2007**, *154*, B652. [CrossRef]
74. Ghassemzadeh, L.; Kreuer, K.-D.; Maier, J.; Müller, K. Chemical Degradation of Nafion Membranes under Mimic Fuel Cell Conditions as Investigated by Solid-State NMR Spectroscopy. *J. Phys. Chem. C* **2010**, *114*, 14635–14645. [CrossRef]
75. Kadirov, M.K.; Bosnjakovic, A.; Schlick, S. Membrane-Derived Fluorinated Radicals Detected by Electron Spin Resonance in UV-Irradiated Nafion and Dow Ionomers: Effect of Counterions and H_2O_2. *J. Phys. Chem. B* **2005**, *109*, 7664–7670. [CrossRef]
76. Coms, F.D. The Chemistry of Fuel Cell Membrane Chemical Degradation. *ECS Trans.* **2008**, *16*, 235. [CrossRef]
77. Ghassemzadeh, L.; Peckham, T.J.; Weissbach, T.; Luo, X.; Holdcroft, S. Selective Formation of Hydrogen and Hydroxyl Radicals by Electron Beam Irradiation and Their Reactivity with Perfluorosulfonated Acid Ionomer. *J. Am. Chem. Soc.* **2013**, *135*, 15923–15932. [CrossRef]
78. Ghassemzadeh, L.; Holdcroft, S. Quantifying the Structural Changes of Perfluorosulfonated Acid Ionomer upon Reaction with Hydroxyl Radicals. *J. Am. Chem. Soc.* **2013**, *135*, 8181–8184. [CrossRef]
79. Long, H.; Larson, C.; Coms, F.; Pivovar, B.; Dahlke, G.; Yandrasits, M. Role of $H_3O\cdot$ Radical in the Degradation of Fuel Cell Proton-Exchange Membranes. *ACS Phys. Chem. Au* **2022**, *2*, 527–534. [CrossRef]
80. Ding, F.; Zou, T.; Wei, T.; Chen, L.; Qin, X.; Shao, Z.; Yang, J. The Pinhole Effect on Proton Exchange Membrane Fuel Cell (PEMFC) Current Density Distribution and Temperature Distribution. *Appl. Energy* **2023**, *342*, 121136. [CrossRef]
81. Jeong, K.I.; Oh, J.; Song, S.A.; Lee, D.; Lee, D.G.; Kim, S.S. A Review of Composite Bipolar Plates in Proton Exchange Membrane Fuel Cells: Electrical Properties and Gas Permeability. *Compos. Struct.* **2021**, *262*, 113617. [CrossRef]
82. Özyalcin, C.; Mauermann, P.; Dirkes, S.; Thiele, P.; Sterlepper, S.; Pischinger, S. Investigation of Filtration Phenomena of Air Pollutants on Cathode Air Filters for PEM Fuel Cells. *Catalysts* **2021**, *11*, 1339. [CrossRef]
83. Yang, D.; Ma, X.; Lv, H.; Li, B.; Zhang, C. NO Adsorption and Temperature Programmed Desorption on K2CO3 Modified Activated Carbons. *J. Cent. South Univ.* **2018**, *25*, 2339–2348. [CrossRef]
84. Oesch, S.; Faller, M. Environmental Effects on Materials: The Effect of the Air Pollutants SO_2, NO_2, NO and O_3 on the Corrosion of Copper, Zinc and Aluminium. A Short Literature Survey and Results of Laboratory Exposures. *Corros. Sci.* **1997**, *39*, 1505–1530. [CrossRef]
85. Molochas, C.; Tsiakaras, P. Carbon Monoxide Tolerant Pt-Based Electrocatalysts for H2-PEMFC Applications: Current Progress and Challenges. *Catalysts* **2021**, *11*, 1127. [CrossRef]
86. Liu, Q.; Zhang, S.; Zhuo, L.; Wang, Z.; Wang, C.; Sun, F.; Niu, K.; Xu, F.; Che, X.; Zhang, J.; et al. Advanced Proton Exchange Membrane Prepared from N-Heterocyclic Poly(Aryl Ether Ketone)s with Pendant Benzenesulfonic Moieties and Performing Enhanced Radical Tolerance and Fuel Cell Properties. *J. Membr. Sci.* **2023**, *681*, 121767. [CrossRef]
87. Wallnöfer-Ogris, E.; Poimer, F.; Köll, R.; Macherhammer, M.-G.; Trattner, A. Main Degradation Mechanisms of Polymer Electrolyte Membrane Fuel Cell Stacks—Mechanisms, Influencing Factors, Consequences, and Mitigation Strategies. *Int. J. Hydrogen Energy* **2024**, *50*, 1159–1182. [CrossRef]
88. Zatoń, M.; Rozière, J.; Jones, D.J. Current Understanding of Chemical Degradation Mechanisms of Perfluorosulfonic Acid Membranes and Their Mitigation Strategies: A Review. *Sustain. Energy Fuels* **2017**, *1*, 409–438. [CrossRef]
89. Liu, W.; Qiu, D.; Peng, L.; Lai, X. Study on the Nonuniform Mechanical Degradation of Membranes Considering Temperature and Relative Humidity Distribution in Proton Exchange Membrane Fuel Cells. *Fuel Cells* **2023**, *23*, 170–180. [CrossRef]
90. De Bruijn, F.A.; Dam, V.A.T.; Janssen, G.J.M. Review: Durability and Degradation Issues of PEM Fuel Cell Components. *Fuel Cells* **2008**, *8*, 3–22. [CrossRef]
91. Qiu, D.; Peng, L.; Liang, P.; Yi, P.; Lai, X. Mechanical Degradation of Proton Exchange Membrane along the MEA Frame in Proton Exchange Membrane Fuel Cells. *Energy* **2018**, *165*, 210–222. [CrossRef]
92. Jouin, M.; Gouriveau, R.; Hissel, D.; Péra, M.-C.; Zerhouni, N. Degradations Analysis and Aging Modeling for Health Assessment and Prognostics of PEMFC. *Reliab. Eng. Syst. Saf.* **2016**, *148*, 78–95. [CrossRef]
93. Patil, Y.P.; Jarrett, W.L.; Mauritz, K.A. Deterioration of Mechanical Properties: A Cause for Fuel Cell Membrane Failure. *J. Membr. Sci.* **2010**, *356*, 7–13. [CrossRef]
94. Shi, S.; Sun, X.; Lin, Q.; Chen, J.; Fu, Y.; Hong, X.; Li, C.; Guo, X.; Chen, G.; Chen, X. Fatigue Crack Propagation Behavior of Fuel Cell Membranes after Chemical Degradation. *Int. J. Hydrogen Energy* **2020**, *45*, 27653–27664. [CrossRef]

95. Kundu, S.; Simon, L.C.; Fowler, M.; Grot, S. Mechanical Properties of Nafion™ Electrolyte Membranes under Hydrated Conditions. *Polymer* **2005**, *46*, 11707–11715. [CrossRef]
96. Tang, H.; Peikang, S.; Jiang, S.P.; Wang, F.; Pan, M. A Degradation Study of Nafion Proton Exchange Membrane of PEM Fuel Cells. *J. Power Sources* **2007**, *170*, 85–92. [CrossRef]
97. Dafalla, A.M.; Jiang, F. Stresses and Their Impacts on Proton Exchange Membrane Fuel Cells: A Review. *Int. J. Hydrogen Energy* **2018**, *43*, 2327–2348. [CrossRef]
98. McDonald, R.C.; Mittelsteadt, C.K.; Thompson, E.L. Effects of Deep Temperature Cycling on Nafion® 112 Membranes and Membrane Electrode Assemblies. *Fuel Cells* **2004**, *4*, 208–213. [CrossRef]
99. Taylor, A.K.; Smith, C.; Neyerlin, K.C. Mitigation and Diagnosis of Pin-Hole Formation in Polymer Electrolyte Membrane Fuel Cells. *J. Power Sources* **2023**, *571*, 232971. [CrossRef]
100. Qiu, D.; Peng, L.; Lai, X.; Ni, M.; Lehnert, W. Mechanical Failure and Mitigation Strategies for the Membrane in a Proton Exchange Membrane Fuel Cell. *Renew. Sustain. Energy Rev.* **2019**, *113*, 109289. [CrossRef]
101. Jiang, F.; Fang, W.; Wang, C.-Y. Non-Isothermal Cold Start of Polymer Electrolyte Fuel Cells. *Electrochim. Acta* **2007**, *53*, 610–621. [CrossRef]
102. Cho, E.; Ko, J.-J.; Ha, H.Y.; Hong, S.-A.; Lee, K.-Y.; Lim, T.-W.; Oh, I.-H. Effects of Water Removal on the Performance Degradation of PEMFCs Repetitively Brought to < 0 °C. *J. Electrochem. Soc.* **2004**, *151*, A661. [CrossRef]
103. Cho, E.; Ko, J.-J.; Ha, H.Y.; Hong, S.-A.; Lee, K.-Y.; Lim, T.-W.; Oh, I.-H. Characteristics of the PEMFC Repetitively Brought to Temperatures below 0 °C. *J. Electrochem. Soc.* **2003**, *150*, A1667. [CrossRef]
104. Frensch, S.H.; Serre, G.; Fouda-Onana, F.; Jensen, H.C.; Christensen, M.L.; Araya, S.S.; Kær, S.K. Impact of Iron and Hydrogen Peroxide on Membrane Degradation for Polymer Electrolyte Membrane Water Electrolysis: Computational and Experimental Investigation on Fluoride Emission. *J. Power Sources* **2019**, *420*, 54–62. [CrossRef]
105. Zhao, J.; Li, X. A Review of Polymer Electrolyte Membrane Fuel Cell Durability for Vehicular Applications: Degradation Modes and Experimental Techniques. *Energy Convers. Manag.* **2019**, *199*, 112022. [CrossRef]
106. Wilkie, C.A.; Thomsen, J.R.; Mittleman, M.L. Interaction of Poly(Methyl Methacrylate) and Nafions. *J. Appl. Polym. Sci.* **1991**, *42*, 901–909. [CrossRef]
107. Pan, M.; Pan, C.; Li, C.; Zhao, J. A Review of Membranes in Proton Exchange Membrane Fuel Cells: Transport Phenomena, Performance and Durability. *Renew. Sustain. Energy Rev.* **2021**, *141*, 110771. [CrossRef]
108. Dafalla, A.M.; Wei, L.; Habte, B.T.; Guo, J.; Jiang, F. Membrane Electrode Assembly Degradation Modeling of Proton Exchange Membrane Fuel Cells: A Review. *Energies* **2022**, *15*, 9247. [CrossRef]
109. Okada, T.; Satou, H.; Yuasa, M. Effects of Additives on Oxygen Reduction Kinetics at the Interface between Platinum and Perfluorinated Ionomer. *Langmuir* **2003**, *19*, 2325–2332. [CrossRef]
110. Collier, A.; Wang, H.; Zi Yuan, X.; Zhang, J.; Wilkinson, D.P. Degradation of Polymer Electrolyte Membranes. *Int. J. Hydrogen Energy* **2006**, *31*, 1838–1854. [CrossRef]
111. Collette, F.M.; Lorentz, C.; Gebel, G.; Thominette, F. Hygrothermal Aging of Nafion®. *J. Membr. Sci.* **2009**, *330*, 21–29. [CrossRef]
112. Ergun, D.; Devrim, Y.; Bac, N.; Eroglu, I. Phosphoric Acid Doped Polybenzimidazole Membrane for High Temperature PEM Fuel Cell. *J. Appl. Polym. Sci.* **2012**, *124*, E267–E277. [CrossRef]
113. Haider, R.; Wen, Y.; Ma, Z.F.; Wilkinson, D.P.; Zhang, L.; Yuan, X.; Song, S.; Zhang, J. High Temperature Proton Exchange Membrane Fuel Cells: Progress in Advanced Materials and Key Technologies. *Chem. Soc. Rev.* **2021**, *50*, 1138–1187. [CrossRef]
114. Chen, Q.; Zhang, G.; Zhang, X.; Sun, C.; Jiao, K.; Wang, Y. Thermal Management of Polymer Electrolyte Membrane Fuel Cells: A Review of Cooling Methods, Material Properties, and Durability. *Appl. Energy* **2021**, *286*, 116496. [CrossRef]
115. Huang, Y.; Xiao, X.; Kang, H.; Lv, J.; Zeng, R.; Shen, J. Thermal Management of Polymer Electrolyte Membrane Fuel Cells: A Critical Review of Heat Transfer Mechanisms, Cooling Approaches, and Advanced Cooling Techniques Analysis. *Energy Convers. Manag.* **2022**, *254*, 115221. [CrossRef]
116. Peng, M.; Chen, L.; Zhang, R.; Xu, W.; Tao, W.-Q. Improvement of Thermal and Water Management of Air-Cooled Polymer Electrolyte Membrane Fuel Cells by Adding Porous Media into the Cathode Gas Channel. *Electrochim. Acta* **2022**, *412*, 140154. [CrossRef]
117. Raguman, A.; Vedagiri, P. A Review on Recent Approaches in Thermal and Water Management of Polymer Electrolyte Membrane Fuel Cells. *Mater. Today Proc.* **2022**, *68*, 1975–1979. [CrossRef]
118. Hooshyari, K.; Amini Horri, B.; Abdoli, H.; Fallah Vostakola, M.; Kakavand, P.; Salarizadeh, P. A Review of Recent Developments and Advanced Applications of High-Temperature Polymer Electrolyte Membranes for PEM Fuel Cells. *Energies* **2021**, *14*, 5440. [CrossRef]
119. Primachenko, O.N.; Marinenko, E.A.; Odinokov, A.S.; Kononova, S.V.; Kulvelis, Y.V.; Lebedev, V.T. State of the Art and Prospects in the Development of Proton-Conducting Perfluorinated Membranes with Short Side Chains: A Review. *Polym. Adv. Technol.* **2021**, *32*, 1386–1408. [CrossRef]
120. Ju, Q.; Chao, G.; Wang, Y.; Lv, Z.; Geng, K.; Li, N. An Antioxidant Polybenzimidazole with Naphthalene Group for High-Temperature Proton Exchange Membrane Fuel Cells. *J. Membr. Sci.* **2023**, *686*, 121970. [CrossRef]
121. Harun, N.A.M.; Shaari, N.; Nik Zaiman, N.F.H. A Review of Alternative Polymer Electrolyte Membrane for Fuel Cell Application Based on Sulfonated Poly(Ether Ether Ketone). *Int. J. Energy Res.* **2021**, *45*, 19671–19708. [CrossRef]

122. Mohamad Nor, N.A.; Mohamed, M.A.; Jaafar, J. Modified Sulfonated Polyphenylsulfone Proton Exchange Membrane with Enhanced Fuel Cell Performance: A Review. *J. Ind. Eng. Chem.* **2022**, *116*, 32–59. [CrossRef]
123. Xu, M.; Xue, H.; Wang, Q.; Jia, L. Sulfonated Poly(Arylene Ether)s Based Proton Exchange Membranes for Fuel Cells. *Int. J. Hydrogen Energy* **2021**, *46*, 31727–31753. [CrossRef]
124. Liu, F.; Miyatake, K. Well-Designed Polyphenylene PEMs with High Proton Conductivity and Chemical and Mechanical Durability for Fuel Cells. *J. Mater. Chem. A* **2022**, *10*, 7660–7667. [CrossRef]
125. Wijaya, F.; Woo, S.; Lee, H.; Nugraha, A.F.; Shin, D.; Bae, B. Sulfonated Poly(Phenylene-Co-Arylene Ether Sulfone) Multiblock Membranes for Application in High-Performance Fuel Cells. *J. Membr. Sci.* **2022**, *645*, 120203. [CrossRef]
126. Karimi, A.; Mirfarsi, S.H.; Rowshanzamir, S.; Beyraghi, F.; Lester, D. Vicious Cycle during Chemical Degradation of Sulfonated Aromatic Proton Exchange Membranes in the Fuel Cell Application. *Int. J. Energy Res.* **2020**, *44*, 8877–8891. [CrossRef]
127. Dahe, G.J.; Singh, R.P.; Dudeck, K.W.; Yang, D.; Berchtold, K.A. Influence of Non-Solvent Chemistry on Polybenzimidazole Hollow Fiber Membrane Preparation. *J. Membr. Sci.* **2019**, *577*, 91–103. [CrossRef]
128. Qu, E.; Hao, X.; Xiao, M.; Han, D.; Huang, S.; Huang, Z.; Wang, S.; Meng, Y. Proton Exchange Membranes for High Temperature Proton Exchange Membrane Fuel Cells: Challenges and Perspectives. *J. Power Sources* **2022**, *533*, 231386. [CrossRef]
129. Guo, Z.; Perez-Page, M.; Chen, J.; Ji, Z.; Holmes, S.M. Recent Advances in Phosphoric Acid–Based Membranes for High–Temperature Proton Exchange Membrane Fuel Cells. *J. Energy Chem.* **2021**, *63*, 393–429. [CrossRef]
130. Jin, Y.; Wang, T.; Che, X.; Dong, J.; Li, Q.; Yang, J. Poly(Arylene Pyridine)s: New Alternative Materials for High Temperature Polymer Electrolyte Fuel Cells. *J. Power Sources* **2022**, *526*, 231131. [CrossRef]
131. Hu, X.; Ao, Y.; Gao, Y.; Liu, B.; Zhao, C. Facile Preparation of Triazole-Functionalized Poly(Arylene Perfluorophenyl) High Temperature Proton Exchange Membranes via Para-Fluoro-Thiol Click Reaction with High Radical Resistance. *J. Membr. Sci.* **2023**, *687*, 122102. [CrossRef]
132. Li, Y.; Xu, S.; Wang, J.; Liu, X.; Yang, Y.; Yang, F.; He, R. Terphenyl Pyridine Based Polymers for Superior Conductivity and Excellent Chemical Stability of High Temperature Proton Exchange Membranes. *Eur. Polym. J.* **2022**, *173*, 111295. [CrossRef]
133. Huang, H.; Zeng, X.; Zhang, X.; Fan, J.; Li, H. Proton Exchange Membrane Based on Interpenetrating Polymer Network Structure for Excellent Cell Performance and Chemical Stability. *J. Power Sources* **2023**, *558*, 232602. [CrossRef]
134. Wang, J.; Dai, Y.; Wan, R.; Wei, W.; Xu, S.; Zhai, F.; He, R. Grafting Free Radical Scavengers onto Polyarylethersulfone Backbones for Superior Chemical Stability of High Temperature Polymer Membrane Electrolytes. *Chem. Eng. J.* **2021**, *413*, 127541. [CrossRef]
135. Agarwal, T.; Adhikari, S.; Kim, Y.S.; Babu, S.K.; Tian, D.; Bae, C.; Pham, N.N.T.; Lee, S.G.; Prasad, A.K.; Advani, S.G.; et al. Fluoroalkyl Phosphonic Acid Radical Scavengers for Proton Exchange Membrane Fuel Cells. *J. Mater. Chem. A* **2023**, *11*, 9748–9754. [CrossRef]
136. Teixeira, F.C.; Teixeira, A.P.S.; Rangel, C.M. Chemical Stability of New Nafion Membranes Doped with Bisphosphonic Acids under Fenton Oxidative Conditions. *Int. J. Hydrogen Energy* **2023**, *48*, 37489–37499. [CrossRef]
137. Son, B.; Oh, K.; Park, S.; Lee, T.-G.; Lee, D.H.; Kwon, O. Study of Morphological Characteristics on Hydrophilicity-Enhanced SiO2/Nafion Composite Membranes by Using Multimode Atomic Force Microscopy. *Int. J. Energy Res.* **2019**, *43*, 4157–4169. [CrossRef]
138. Maiti, T.K.; Singh, J.; Dixit, P.; Majhi, J.; Bhushan, S.; Bandyopadhyay, A.; Chattopadhyay, S. Advances in Perfluorosulfonic Acid-Based Proton Exchange Membranes for Fuel Cell Applications: A Review. *Chem. Eng. J. Adv.* **2022**, *12*, 100372. [CrossRef]
139. Zhang, X.; Yu, S.; Zhu, Q.; Zhao, L. Enhanced Anhydrous Proton Conductivity of SPEEK/IL Composite Membrane Embedded with Amino Functionalized Mesoporous Silica. *Int. J. Hydrogen Energy* **2019**, *44*, 6148–6159. [CrossRef]
140. Zhao, D.; Yi, B.L.; Zhang, H.M.; Yu, H.M. MnO_2/SiO_2–SO_3H Nanocomposite as Hydrogen Peroxide Scavenger for Durability Improvement in Proton Exchange Membranes. *J. Membr. Sci.* **2010**, *346*, 143–151. [CrossRef]
141. Gashoul, F.; Parnian, M.J.; Rowshanzamir, S. A New Study on Improving the Physicochemical and Electrochemical Properties of SPEEK Nanocomposite Membranes for Medium Temperature Proton Exchange Membrane Fuel Cells Using Different Loading of Zirconium Oxide Nanoparticles. *Int. J. Hydrogen Energy* **2017**, *42*, 590–602. [CrossRef]
142. Khalifa, R.E.; Omer, A.M.; Abd Elmageed, M.H.; Mohy Eldin, M.S. Titanium Dioxide/Phosphorous-Functionalized Cellulose Acetate Nanocomposite Membranes for DMFC Applications: Enhancing Properties and Performance. *ACS Omega* **2021**, *6*, 17194–17202. [CrossRef]
143. Chandra Kishore, S.; Perumal, S.; Atchudan, R.; Alagan, M.; Wadaan, M.A.; Baabbad, A.; Manoj, D. Recent Advanced Synthesis Strategies for the Nanomaterial-Modified Proton Exchange Membrane in Fuel Cells. *Membranes* **2023**, *13*, 590. [CrossRef]
144. Vandeginste, V.; Madhav, D. Interface Modification and Characterization of PVC Based Composites and Nanocomposites. In *Poly (Vinyl Chloride) Based Composites and Nanocomposites*; Engineering Materials; H, A., Sabu, T., Eds.; Springer International Publishing: Cham, Switzerland, 2024; pp. 55–86. ISBN 978-3-031-45375-5.
145. Vinothkannan, M.; Hariprasad, R.; Ramakrishnan, S.; Kim, A.R.; Yoo, D.J. Potential Bifunctional Filler (CeO_2–ACNTs) for Nafion Matrix toward Extended Electrochemical Power Density and Durability in Proton-Exchange Membrane Fuel Cells Operating at Reduced Relative Humidity. *ACS Sustain. Chem. Eng.* **2019**, *7*, 12847–12857. [CrossRef]
146. Maiti, T.K.; Singh, J.; Maiti, S.K.; Majhi, J.; Ahuja, A.; Singh, M.; Bandyopadhyay, A.; Manik, G.; Chattopadhyay, S. Molecular Dynamics Simulations and Experimental Studies of the Perfluorosulfonic Acid-Based Composite Membranes Containing Sulfonated Graphene Oxide for Fuel Cell Applications. *Eur. Polym. J.* **2022**, *174*, 111345. [CrossRef]

147. Rambabu, G.; Nagaraju, N.; Bhat, S.D. Functionalized Fullerene Embedded in Nafion Matrix: A Modified Composite Membrane Electrolyte for Direct Methanol Fuel Cells. *Chem. Eng. J.* **2016**, *306*, 43–52. [CrossRef]
148. Postnov, V.N.; Mel'nikova, N.A.; Shul'meister, G.A.; Novikov, A.G.; Murin, I.V.; Zhukov, A.N. Nafion- and Aquivion-Based Nanocomposites Containing Detonation Nanodiamonds. *Russ J Gen Chem* **2017**, *87*, 2754–2755. [CrossRef]
149. Madhav, D.; Malankowska, M.; Coronas, J. Synthesis of Nanoparticles of Zeolitic Imidazolate Framework ZIF-94 Using Inorganic Deprotonators. *New J. Chem.* **2020**, *44*, 20449–20457. [CrossRef]
150. Li, X.-M.; Gao, J. Recent Advances of Metal–Organic Frameworks-Based Proton Exchange Membranes in Fuel Cell Applications. *SusMat* **2022**, *2*, 504–534. [CrossRef]
151. Khoo, K.S.; Chia, W.Y.; Wang, K.; Chang, C.-K.; Leong, H.Y.; Maaris, M.N.B.; Show, P.L. Development of Proton-Exchange Membrane Fuel Cell with Ionic Liquid Technology. *Sci. Total Environ.* **2021**, *793*, 148705. [CrossRef] [PubMed]
152. Alashkar, A.; Al-Othman, A.; Tawalbeh, M.; Qasim, M. A Critical Review on the Use of Ionic Liquids in Proton Exchange Membrane Fuel Cells. *Membranes* **2022**, *12*, 178. [CrossRef] [PubMed]
153. Rui, Z.; Liu, J. Understanding of Free Radical Scavengers Used in Highly Durable Proton Exchange Membranes. *Prog. Nat. Sci. Mater. Int.* **2020**, *30*, 732–742. [CrossRef]
154. Liu, L.; Xing, Y.; Li, Y.; Fu, Z.; Li, Z.; Li, H. Double-Layer Expanded Polytetrafluoroethylene Reinforced Membranes with Cerium Oxide Radical Scavengers for Highly Stable Proton Exchange Membrane Fuel Cells. *ACS Appl. Energy Mater.* **2022**, *5*, 8743–8755. [CrossRef]
155. Ram, F.; Velayutham, P.; Sahu, A.K.; Lele, A.K.; Shanmuganathan, K. Enhancing Thermomechanical and Chemical Stability of Polymer Electrolyte Membranes Using Polydopamine Coated Nanocellulose. *ACS Appl. Energy Mater.* **2020**, *3*, 1988–1999. [CrossRef]
156. Tinh, V.D.C.; Thuc, V.D.; Kim, D. Chemically Sustainable Fuel Cells via Layer-by-Layer Fabrication of Sulfonated Poly(Arylene Ether Sulfone) Membranes Containing Cerium Oxide Nanoparticles. *J. Membr. Sci.* **2021**, *634*, 119430. [CrossRef]
157. Xu, K.; Pei, S.; Zhang, W.; Han, Z.; Liu, G.; Xu, X.; Ma, J.; Zhang, Y.; Liu, F.; Zhang, Y.; et al. Chemical Stability of Proton Exchange Membranes Synergistically Promoted by Organic Antioxidant and Inorganic Radical Scavengers. *J. Membr. Sci.* **2022**, *655*, 120594. [CrossRef]
158. Agarwal, T.; Sievert, A.C.; Komini Babu, S.; Adhikari, S.; Park, E.J.; Prasad, A.K.; Advani, S.G.; Hopkins, T.E.; Park, A.M.; Kim, Y.S.; et al. Enhancing Durability of Polymer Electrolyte Membrane Using Cation Size Selective Agents. *J. Power Sources* **2023**, *580*, 233362. [CrossRef]
159. Xu, Y.; Liang, X.; Shen, X.; Yu, W.; Yang, X.; Li, Q.; Ge, X.; Wu, L.; Xu, T. In Situ Construction of Ultra-Thin PANI/CeOx Layer on Proton Exchange Membrane for Enhanced Oxidation Resistance in PEMFC. *J. Membr. Sci.* **2024**, *689*, 122167. [CrossRef]
160. Zhiyan, R.; Qingbing, L.; Youxiu, H.; Rui, D.; Jia, L.; Jia, L.; Jianguo, L. Ceria Nanorods as Highly Stable Free Radical Scavengers for Highly Durable Proton Exchange Membranes. *RSC Adv.* **2021**, *11*, 32012–32021. [CrossRef]
161. Liu, X.; Li, Y.; Li, M.; Xie, N.; Zhang, J.; Qin, Y.; Yin, Y.; Guiver, M.D. Durability Enhancement of Proton Exchange Membrane Fuel Cells by Ferrocyanide or Ferricyanide Additives. *J. Membr. Sci.* **2021**, *629*, 119282. [CrossRef]
162. Zhang, X.; Li, Y.; Liu, X.; Zhang, J.; Yin, Y.; Guiver, M.D. A Paradigm Shift for a New Class of Proton Exchange Membranes with Ferrocyanide Proton-Conducting Groups Providing Enhanced Oxidative Stability. *J. Membr. Sci.* **2020**, *616*, 118536. [CrossRef]
163. Shen, X.; Liang, X.; Xu, Y.; Yu, W.; Li, Q.; Ge, X.; Wu, L.; Xu, T. In-Situ Growth of PPy/MnOx Radical Quenching Layer for Durability Enhancement of Proton Exchange Membrane in PEMFCs. *J. Membr. Sci.* **2023**, *675*, 121556. [CrossRef]